# HIGH-ORDER ACCURATE TIME-STEPPING SCHEMES FOR CONVECTION-DIFFUSION PROBLEMS

J. Donea*, B. Roig † and A. Huerta †

* Aerospace Laboratory-Thermomechanics, University of Liège,
rue E. Solvay, 21, B-4000 Liège, Belgium.

† Universitat Politècnica de Catalunya, Campus Nord Edifici C-2,
Jordi Girona 1, E-08034 Barcelona, Spain.

**Abstract**

The paper discusses the formulation of high-order accurate time-stepping schemes for transient convection-diffusion problems to be combined with finite element methods of the least-squares type for a stable discretization of highly convective problems. Padé approximations of the exponential function are considered for deriving multi-stage time integration schemes involving first time derivatives only, thus easier to implement in conjunction with $C^0$ finite elements than standard time-stepping schemes which incorporate higher order time derivatives. After a brief discussion of the stability and accuracy properties of the multi-stage Padé schemes and having underlined the similarity between Padé and Runge-Kutta methods, the paper closes with the presentation of illustrative examples which indicate the effectiveness of the proposed methods.

**Key words:** Convection-Diffusion, Time-Stepping Schemes, Padé Approximants, Finite Elements

## 1 INTRODUCTION

A great deal of effort has been devoted in recent years to the development of finite element methods for the numerical approximation of transport problems involving convective and diffusive processes. It is well-known that the standard Galerkin finite element method is not ideally suited to deal with

the spatial discretization of convection dominated transport problems. Many different ideas and approaches have been proposed to overcome the deficiencies of the Galerkin approach in highly convective situations, see for instance the recent book by K.W. Morton[1] for a comprehensive review of the various strategies proposed to deal with highly convective transport.

In the particular case of truly transient problems, which is of interest in the present paper, the basic issue is not merely a question of achieving a stable and accurate spatial approximation of the governing convection-diffusion equation, another equally important aspect being to ensure an adequate coupling between the spatial approximation provided by the finite element method and the time discretization.[2–5] In this respect, it has been shown that the combination of a standard Galerkin spatial discretization with classical, second-order accurate, time-stepping schemes, such as the Lax-Wendroff, leap-frog, and Crank-Nicolson methods, fails to produce satisfactory numerical results when convection dominates the transport process. Actually, the above low-order time integration methods properly combine with linear finite elements in convection problems only for small values of the time step, thus severely undermining the utility of such time integration schemes in practical applications.

Moreover, two other important issues motivate the use of high-order integration schemes. On one hand, the high order spatial approximation afforded by the Galerkin method based upon linear elements should not be degraded by the use of a low order temporal approximation. It is in fact well known (as first pointed out by Swartz[6] and Thomée and Wendroff[7] in 1974) that the Galerkin approximation to the unsteady convection equation on a uniform mesh of linear elements offers the advantage of increasing to fourth-order the spatial accuracy. This is a free gift due to the presence of a consistent mass matrix in the Galerkin method. On the other hand, the computational cost of transient problems is directly related to the size of the time step. Thus, increasing the order of the time-stepping algorithm allows to use larger time steps maintaining the overall accuracy (which, obviously, must be comparable to the spatial accuracy). For instance, moving from order 2 to 4 in the time integration scheme implies an increase of the time step size by a factor of $1/\sqrt{\Delta t}$ (where $\Delta t$ is the time step employed in the second order method). This can only be done if the properties of the higher order algorithm (for instance, stability) are not degraded. Here, high-order implicit time-stepping schemes are proposed which adequately combine with $C^0$ finite elements in convection dominated problems because of their simultaneous A-stability and high order accuracy.

Due to the coupling effects between space and time discretizations, methods for developing time-accurate finite element methods for highly convective

problems must clearly go beyond the concept of properly adding diffusion to the under-diffusive Galerkin method, which was the key to the success in steady state situations. In the transient case, the overall truncation error of numerical schemes incorporates the effects of both the spatial and the temporal discretizations and this must be taken into account when generalizing the Galerkin finite element method for truly transient problems. In particular, by contrast with the steady state case, the truncation error in the discretization of the linear, one-dimensional convection equation cannot be expressed in the form of a diffusion operator. Here, the overall truncation error depends upon the particular time-stepping method used in combination with finite elements[1,3–5] and it generally involves both even and odd spatial derivatives of the unknown, thus simultaneously affecting the dissipative and the dispersive properties of the numerical schemes.

In the present paper, a study has been made of high order time-stepping methods with the view of identifying schemes that could possibly be used for a time accurate finite element solution of transient problems describing convective-diffusive transport. Both explicit and implicit methods are considered.

To be easily implemented in combination with $C^0$ finite elements, high-order time-stepping schemes for the convection-diffusion equation should not involve higher-order time derivatives. This is the case for multi-stage schemes emanating from Padé approximations to the exponential function,[8,9] as well as for the intimately related Runge-Kutta methods.[10,12] Schemes involving first time derivatives are indeed easier to implement for solving unsteady convection-diffusion problems than, for instance, the standard third- and fourth-order accurate Taylor-Galerkin schemes which imply the substitution of the higher order time derivatives with spatial derivatives.[13] Moreover, some of the implicit methods to be discussed in the present paper possess the interesting property of unconditional stability in application to hybrid parabolic-hyperbolic equations and are thus of great interest for solving transient convection-diffusion problems using time increments much larger than permitted by the Courant stability limit of explicit methods.

Section 2 is devoted to the derivation of explicit and implicit multi-stage time integration schemes obtained from Padé approximations to the exponential function. Such schemes are combined with a least-squares type finite element method free of any extra adjustable parameter (only the usual ones associated with the time and space discretization, $\Delta t$ and $h$, are employed) with the view of producing stable approximations of highly convective problems.

Section 3 gives a brief overview of the properties of explicit and implicit Padé methods as regards numerical stability and phase and damping re-

sponses. After underlining in Section 4 the similarities between Padé schemes and Runge-Kutta methods, numerical results are presented in Section 5 to confirm the accuracy and stability properties of some of the multi-stage methods considered in the paper. In particular, a new two-dimensional Burgers test problem is presented for which the analytical solution has been devised, thus allowing a direct assessment of the numerical results.

Finally, Section 6 presents the main conclusions of the present study.

# 2 MULTI-STAGE APPROACH TO PADE APPROXIMATIONS

Consider the convection-diffusion equation

$$\frac{\partial u}{\partial t} + \boldsymbol{a} \cdot \nabla \mathbf{u} = \nu \nabla^{\mathbf{2}} \mathbf{u} + \mathbf{f}, \tag{1}$$

equipped with appropriate initial and boundary conditions. Here, $\boldsymbol{a}$ designates the convection velocity, $\nu$ is the diffusion coefficient, and $f$ a source term.

The task of integrating forward in time the above convection-diffusion equation amounts to devise an approximation to the evolution operator

$$E(\Delta t) \, : \, u(t^n) \, \rightarrow \, u(t^{n+1})$$

which allows to transport the numerical solution at a given time $t^n = n\,\Delta t$ to the next time station $t^{n+1} = t^n + \Delta t$. Now, from the forward Taylor series development

$$\begin{aligned} u^{n+1} &= \left(1 + \Delta t \frac{\partial}{\partial t} + \frac{1}{2!}\Delta t^2 \frac{\partial^2}{\partial t^2} + \frac{1}{3!}\Delta t^3 \frac{\partial^3}{\partial t^3} + \ldots\right) u^n \\ &= \exp\left(\Delta t \frac{\partial}{\partial t}\right) u^n, \end{aligned} \tag{2}$$

one notes that the evolution operator $E(\Delta t)$ is given by the exponential function in the above relationship. It is, therefore, apparent that time-stepping schemes of various orders of accuracy can be devised in the form of Padé approximations[8,9,12] to the exponential function. Padé approximations to $e^x$, where in the present context $x = \Delta t \frac{\partial}{\partial t}$, are shown in Table 1 in which classical explicit and implicit time integration methods are easily recognized.

| $R_{n,m}(x)$ | $n=0$ | $n=1$ | $n=2$ | $n=3$ |
|---|---|---|---|---|
| $m=0$ | $1$ | $1+x$ | $1+x+\frac{1}{2}x^2$ | $1+x+\frac{1}{2}x^2+\frac{1}{6}x^3$ |
| $m=1$ | $\frac{1}{1-x}$ | $\frac{1+\frac{1}{2}x}{1-\frac{1}{2}x}$ | $\frac{1+\frac{2}{3}x+\frac{1}{6}x^2}{1-\frac{1}{3}x}$ | $\frac{1+\frac{3}{4}x+\frac{1}{4}x^2+\frac{1}{24}x^3}{1-\frac{1}{4}x}$ |
| $m=2$ | $\frac{1}{1-x+\frac{1}{2}x^2}$ | $\frac{1+\frac{1}{3}x}{1-\frac{2}{3}x+\frac{1}{6}x^2}$ | $\frac{1+\frac{1}{2}x+\frac{1}{12}x^2}{1-\frac{1}{2}x+\frac{1}{12}x^2}$ | $\frac{1+\frac{3}{5}x+\frac{3}{20}x^2+\frac{1}{60}x^3}{1-\frac{2}{5}x+\frac{1}{20}x^2}$ |
| $m=3$ | $\frac{1}{1-x+\frac{1}{2}x^2-\frac{1}{6}x^3}$ | $\frac{1+\frac{1}{4}x}{1-\frac{3}{4}x+\frac{1}{4}x^2-\frac{1}{24}x^3}$ | $\frac{1+\frac{2}{5}x+\frac{1}{20}x^2}{1-\frac{3}{5}x+\frac{3}{20}x^2-\frac{1}{60}x^3}$ | $\frac{1+\frac{1}{2}x+\frac{1}{10}x^2+\frac{1}{120}x^3}{1-\frac{1}{2}x+\frac{1}{10}x^2-\frac{1}{120}x^3}$ |

Table 1: Padé approximations of the exponential function $e^x$.

## 2.1 Limitations of one-step Padé methods

Explicit time-stepping schemes correspond to Padé approximants $R_{n,0}$ in Table 1. Among these conditionally stable methods, approximant $R_{2,0}$, the Lax-Wendroff method, and the third-order scheme $R_{3,0}$ have been widely used in the numerical simulation of convective transport problems. The classical implementation of these methods consists of replacing the successive time derivatives in Eq.(2) by all the terms left in Eq.(1), in particular, the spatial derivatives. Then, the time-discrete scheme is discretized in space using, for instance, the standard Galerkin finite element method.

In application to pure convection, approximant $R_{2,0}$ does not properly combine with linear elements when a consistent "mass" matrix is used. Its numerical stability in 1D is in fact governed by a restricted Courant condition, namely $c^2 \leq 1/3$ where $c$ is the Courant number, as compared to $c^2 \leq 1$ for central finite differences. By contrast, the combination of approximant $R_{3,0}$ and linear finite elements leads to the one-step Taylor-Galerkin method[3] which is stable in 1D for $c^2 \leq 1$, thus indicating that the finite element equivalent of the Lax-Wendroff finite difference method is a third order method.

As regards to implicit schemes, the unconditionally stable methods corresponding to approximation $R_{1,1}$ (the Crank-Nicolson scheme), as well as the fourth-order method derived from approximant $R_{2,2}$ (the Harten/Tal-Ezer method[17]) have also been widely used for solving convective transport problems. Here again, the time derivatives in Padé approximants are replaced by space derivatives to formulate the temporal discretization. The time-stepping schemes so obtained are non-dissipative in pure convection. They must therefore be combined with a Petrov-Galerkin formulation, such as the SUPG,[18] the Galerkin/Least-squares,[19] or the Taylor/Least-squares[21,22] methods in order to obtain a stable spatial representation.

When applied to purely convective problems, the above one-step Padé methods are clearly limited to a third order time accuracy in the case of explicit schemes and to a fourth order accuracy when an implicit method is employed. In fact, they are based on the substitution of time derivatives with spatial derivatives; thus, Padé schemes of higher accuracy would incorporate third and higher order spatial derivatives, which would prevent the use of $C^0$ finite elements for space discretization. Furthermore, the process of replacing time derivatives with spatial derivatives becomes very much involved in the case of multidimensional nonlinear problems.

The situation is even worse when it comes to solving mixed convection-diffusion problems, since the presence of second spatial derivatives in the governing equation further reduces the applicability of one-step Padé meth-

ods. It follows that time-stepping schemes of higher accuracy for convection-diffusion equations should involve first time derivatives only to allow their combination with the standard finite element method.

## 2.2 Multi-stage approach

With the view of integrating convection-diffusion equations forward in time using first time derivatives only, we shall now look at ways of reproducing higher-order Padé approximations through a multi-stage process. Explicit methods will be considered first; then, multi-stage schemes corresponding to implicit Padé approximations will be examined. This is followed in Section 3 by the presentation of a summarized account of the accuracy and stability properties of the various multi-stage Padé schemes.

### 2.2.1 Explicit multi-stage methods

Padé approximants $R_{n,0}$ in the first row of Table 1 yield fully explicit time-stepping schemes of the type:

$$u^{n+1} = E_\Delta\, u^n = u^n + \Delta t\, u_t^n + \frac{1}{2}\Delta t^2\, u_{tt}^n + \frac{1}{6}\Delta t^3\, u_{ttt}^n + \cdots. \qquad (3)$$

To avoid second and higher-order time derivatives which are difficult to express in terms of the spatial derivatives using the governing convection-diffusion equation, a multi-step approach to the explicit schemes derived from the $R_{n,0}$ approximations has been proposed in the literature.

Second-order method

As far as the second order approximant $R_{2,0}$ is concerned, a two-step approach has first been suggested by Richtmyer in the finite difference context (see reference 14). Here, we write the two-step version of the scheme in the form

$$\left\{ \begin{array}{rcl} u^{n+\frac{1}{2}} & = & u^n + \frac{1}{2}\Delta t\, u_t^n \\ u^{n+1} & = & u^n + \Delta t\, u_t^{n+\frac{1}{2}} \end{array} \right. \qquad (4)$$

which emanates from the following nested factorization of Padé approximation $R_{2,0}$:

$$1 + x + \frac{1}{2}x^2 = 1 + x\left(1 + \frac{1}{2}x\right) \qquad (5)$$

Third-order method

Similarly, for Padé approximation $R_{3,0}$, a three-stage approach has been suggested to produce a third-order method involving first time derivatives

only. This corresponds to the following factorization of $R_{3,0}$:

$$1 + x + \frac{1}{2}x^2 + \frac{1}{6}x^3 = 1 + x\left(1 + \frac{1}{2}x(1 + \frac{1}{3}x)\right) \tag{6}$$

which produces the three-stage scheme

$$\left\{ \begin{array}{rcl} u^{n+\frac{1}{3}} & = & u^n + \frac{1}{3}\Delta t\, u_t^n \\ u^{n+\frac{1}{2}} & = & u^n + \frac{1}{2}\Delta t\, u_t^{n+\frac{1}{3}} \\ u^{n+1} & = & u^n + \Delta t\, u_t^{n+\frac{1}{2}} \end{array} \right. \tag{7}$$

This third-order explicit scheme has been employed in references 15 and 16 in the finite element solution of incompressible flow problems.

**Fourth-order method**

The above procedure is easily generalized to higher order Padé approximants. For instance, the explicit Padé approximation $R_{4,0}$ can be transformed into a four-stage method through the following factorization:

$$1 + x + \frac{1}{2}x^2 + \frac{1}{6}x^3 + \frac{1}{24}x^4 = 1 + x\left(1 + \frac{1}{2}x\left(1 + \frac{1}{3}x(1 + \frac{1}{4}x)\right)\right) \tag{8}$$

which produces the four-stage explicit method

$$\left\{ \begin{array}{rcl} u^{n+\frac{1}{4}} & = & u^n + \frac{1}{4}\Delta t\, u_t^n \\ u^{n+\frac{1}{3}} & = & u^n + \frac{1}{3}\Delta t\, u_t^{n+\frac{1}{4}} \\ u^{n+\frac{1}{2}} & = & u^n + \frac{1}{2}\Delta t\, u_t^{n+\frac{1}{3}} \\ u^{n+1} & = & u^n + \Delta t\, u_t^{n+\frac{1}{2}} \end{array} \right. \tag{9}$$

As will be seen in Section 3, this method does possess the same stability and accuracy properties as the classical fourth-order explicit Runge-Kutta method.

**Spatial representation**

In the above multi-stage schemes, the spatial discretization of the various time-discretized equations can be performed according to standard finite element procedures. Let us write a typical stage equation corresponding to Eq.(1) with assumed Dirichlet boundary conditions in the form

$$\frac{u^{n+\alpha} - u^n}{\alpha\Delta t} = u_t^{n+\beta} = -\boldsymbol{a}\cdot\nabla\mathbf{u}^{\mathbf{n}+\beta} + \nu\nabla^{\mathbf{2}}\mathbf{u}^{\mathbf{n}+\beta} + \mathbf{f}^{\mathbf{n}+\beta}. \tag{10}$$

Denoting by $\varphi \in H_0^1(\Omega)$ an appropriate weighting function, and introducing the scalar product $(\psi, \varphi) = \int_\Omega \psi\, \varphi\, d\Omega$, the weak form associated with Eq.(10) reads

$$\left(\frac{u^{n+\alpha} - u^n}{\alpha\Delta t}, \varphi\right) + a\left(u^{n+\beta}, \varphi\right) = (f^{n+\beta}, \varphi) \tag{11}$$

where

$$a\left(u^{n+\beta},\varphi\right) = \left(\boldsymbol{a}\cdot\nabla\mathbf{u}^{\mathbf{n}+\beta},\varphi\right) + \left(\nu\nabla\mathbf{u}^{\mathbf{n}+\beta},\nabla\varphi\right). \tag{12}$$

The spatial discretization of the weak form (11) then produces the system of equations governing the updated values $u^{n+\alpha}$ of the unknown. At this point it should be clear that the boundary conditions of the convection-diffusion problems must be enforced at each stage of the time integration procedure. The above explicit multi-stage methods are only conditionally stable and their stability properties shall be briefly discussed in Section 3.

### 2.2.2 Implicit multi-stage methods

We shall now consider implicit multi-stage methods for the convection-diffusion equation emanating from Padé approximations in Table 1 corresponding to $m \neq 0$. Actually, not all implicit methods with $m \neq 0$ are unconditionally stable in application to the linear convection–diffusion equation. As discussed in Section 3, only those approximations which are on or below the diagonal in Table 1, i.e., the $R_{n,m}$ with $m \geq n$, do possess interesting stability properties.

Due to space limitation, we shall limit ourselves to illustrate the derivation of multi-stage implicit Padé schemes for the fourth-order approximant $R_{2,2}$ and the sixth-order one $R_{3,3}$. Multi-stage schemes corresponding to other implicit approximants are derived along similar lines.[9]

**Fourth-order method**

The implicit method corresponding to $R_{2,2}$ reads

$$\left(1 - \frac{x}{2} + \frac{x^2}{12}\right) u^{n+1} = \left(1 + \frac{x}{2} + \frac{x^2}{12}\right) u^n, \tag{13}$$

and produces the well-known fourth-order scheme of Harten and Tal-Ezer:[17]

$$u^{n+1} = u^n + \frac{\Delta t}{2}\left(u_t^n + u_t^{n+1}\right) + \frac{\Delta t^2}{12}\left(u_{tt}^n - u_{tt}^{n+1}\right) \tag{14}$$

To avoid second time derivatives, we rewrite expression (13) in the following factorized form:

$$\left(1 - \frac{x}{2}(1 - \frac{x}{6})\right) u^{n+1} = \left(1 + \frac{x}{2}(1 + \frac{x}{6})\right) u^n \tag{15}$$

from which the following 4-stage method incorporating two explicit stages

and two implicit ones can be deduced:

$$\begin{array}{l} \text{explicit stages} \left\{ \begin{array}{rcl} u^{n+\frac{1}{6}} & = u^n + \frac{\Delta t}{6}\, u_t^n \\ u^{n+\frac{1}{2}} & = u^n + \frac{\Delta t}{2}\, u_t^{n+\frac{1}{6}} \end{array} \right. \\ \text{implicit stages} \left\{ \begin{array}{rcl} u^{n+\frac{5}{6}} - u^{n+1} & = -\frac{\Delta t}{6}\, u_t^{n+1} \\ u^{n+1} & = \frac{\Delta t}{2} u_t^{n+\frac{5}{6}} + u^{n+\frac{1}{2}} \end{array} \right. \end{array} \tag{16}$$

Note that the two implicit stages in (16) are coupled and thus require a simultaneous solution.

The weak forms associated with the above explicit stages are given by

$$\begin{array}{rcl} (u^{n+\frac{1}{6}}, \varphi) & = (u^n, \varphi) + \frac{\Delta t}{6} \left[ (f^n, \varphi) - a(u^n, \varphi) \right] \\ (u^{n+\frac{1}{2}}, \varphi) & = (u^n, \varphi) + \frac{\Delta t}{2} \left[ (f^{n+\frac{1}{6}}, \varphi) - a(u^{n+\frac{1}{6}}, \varphi) \right] \end{array} \tag{17}$$

We associate the following incremental unknowns

$$\boldsymbol{\Delta U} = \left\{ \begin{array}{c} \Delta u^{n+\frac{5}{6}} \\ \Delta u^{n+1} \end{array} \right\} = \left\{ \begin{array}{c} u^{n+\frac{5}{6}} - u^{n+\frac{1}{2}} \\ u^{n+1} - u^{n+\frac{5}{6}} \end{array} \right\} \tag{18}$$

with the implicit stages in Eq.(16), which then become

$$\boldsymbol{\Delta U} = \Delta t\, \mathbf{A}\, \boldsymbol{\Delta U}_t + \mathbf{F}, \tag{19}$$

where

$$\begin{array}{rcl} \mathbf{A} & = & \frac{1}{6} \left[ \begin{array}{cc} 2 & -1 \\ 1 & 1 \end{array} \right], \\ \boldsymbol{F} & = & \frac{\Delta t}{6} \left\{ \begin{array}{c} 2 \\ 1 \end{array} \right\} \left( -\boldsymbol{a} \cdot \nabla \mathbf{u}^{\mathbf{n+\frac{1}{2}}} + \nu \nabla^{\mathbf{2}} \mathbf{u}^{\mathbf{n+\frac{1}{2}}} + \mathbf{f}^{\mathbf{n+\frac{1}{2}}} \right). \end{array} \tag{20}$$

After substitution of the time derivatives in Eq.(19) by the original equation, Eq.(1), (i.e. substituting time derivatives with spatial derivatives) we obtain the following weak form corresponding to the two implicit stages

$$(\boldsymbol{\Delta U}, \boldsymbol{\varphi}) - b(\boldsymbol{\Delta U}, \boldsymbol{\varphi}) - l(\boldsymbol{\Delta f}, \boldsymbol{\varphi}) - (\boldsymbol{F}, \boldsymbol{\varphi}) = 0, \tag{21}$$

where

$$\begin{array}{rcl} b(\boldsymbol{\Delta U}, \boldsymbol{\varphi}) & = & \Delta t \int_\Omega \boldsymbol{\varphi} \cdot \mathbf{A} \left[ -\boldsymbol{a} \cdot \nabla \boldsymbol{\Delta U} + \nu \nabla^{\mathbf{2}} \boldsymbol{\Delta U} \right] d\Omega, \\ l(\boldsymbol{\Delta f}, \boldsymbol{\varphi}) & = & \Delta t \int_\Omega \boldsymbol{\varphi} \cdot \mathbf{A}\, \boldsymbol{\Delta f}\, d\Omega, \\ \boldsymbol{\Delta f} & = & \left\{ \begin{array}{c} \Delta f^{n+\frac{5}{6}} \\ \Delta f^{n+1} \end{array} \right\} = \left\{ \begin{array}{c} f^{n+\frac{5}{6}} - f^{n+\frac{1}{2}} \\ f^{n+1} - f^{n+\frac{5}{6}} \end{array} \right\}, \end{array} \tag{22}$$

and $\boldsymbol{\varphi} \in \left(\boldsymbol{H}_0^1(\Omega)\right)^2$.

A more compact formulation of the multi-stage $R_{2,2}$ scheme can be obtained through a fourth-order generalization of Simpson's integration rule.[9] The result reads as follows:

$$\begin{aligned} \boldsymbol{\Delta U} &= \left\{ \begin{array}{c} \Delta u^{n+\frac{1}{2}} \\ \Delta u^{n+1} \end{array} \right\} = \left\{ \begin{array}{c} u^{n+\frac{1}{2}} - u^n \\ u^{n+1} - u^{n+\frac{1}{2}} \end{array} \right\} \\ &= \frac{\Delta t}{24} \left[ \begin{array}{ccc} 5 & 8 & -1 \\ -1 & 8 & 5 \end{array} \right] \left\{ \begin{array}{c} u_t^n \\ u_t^{n+\frac{1}{2}} \\ u_t^{n+1} \end{array} \right\} \end{aligned} \tag{23}$$

and the associated weak form is again given by Eq.(21) with the following definitions

$$\begin{aligned} \mathbf{A} &= \frac{1}{24} \left[ \begin{array}{cc} 7 & -1 \\ 13 & 5 \end{array} \right], \quad \boldsymbol{\Delta f} = \left\{ \begin{array}{c} \Delta f^{n+\frac{1}{2}} \\ \Delta f^{n+1} \end{array} \right\} = \left\{ \begin{array}{c} f^{n+\frac{1}{2}} - f^n \\ f^{n+1} - f^{n+\frac{1}{2}} \end{array} \right\} \\ \boldsymbol{F} &= \frac{\Delta t}{2} \left\{ \begin{array}{c} 1 \\ 1 \end{array} \right\} \left( -\boldsymbol{a} \cdot \nabla \mathbf{u^n} + \nu \nabla^{\mathbf{2}} \mathbf{u^n} + \mathbf{f^n} \right). \end{aligned} \tag{24}$$

**Sixth-order method**

Considering now approximation $R_{3,3}$, it produces the time scheme

$$\left(1 - \frac{x}{2} + \frac{x^2}{10} - \frac{x^3}{120}\right) u^{n+1} = \left(1 + \frac{x}{2} + \frac{x^2}{10} + \frac{x^3}{120}\right) u^n, \tag{25}$$

which reads

$$\frac{u^{n+1} - u^n}{\Delta t} = \frac{1}{2}\left(u_t^n + u_t^{n+1}\right) + \frac{\Delta t}{10}\left(u_{tt}^n - u_{tt}^{n+1}\right) + \frac{\Delta t^2}{120}\left(u_{ttt}^n + u_{ttt}^{n+1}\right), \tag{26}$$

Scheme (26) is sixth-order accurate in the time step $\Delta t$. To implement it using first time derivatives only, the following nested factorization of expression (25) is introduced

$$\left(1 - \frac{x}{2}\left(1 - \frac{x}{5}(1 - \frac{x}{12})\right)\right) u^{n+1} = \left(1 + \frac{x}{2}\left(1 + \frac{x}{5}(1 + \frac{x}{12})\right)\right) u^n \tag{27}$$

This leads to a multi-stage version of $R_{3,3}$ involving three explicit stages

followed by three implicit ones:

$$\text{explicit stages}\begin{cases} u^{n+\frac{1}{12}} &= u^n + \frac{\Delta t}{12}u_t^n \\ u^{n+\frac{1}{5}} &= u^n + \frac{\Delta t}{5}u_t^{n+\frac{1}{12}} \\ u^{n+\frac{1}{2}} &= u^n + \frac{\Delta t}{2}u_t^{n+\frac{1}{5}} \end{cases}$$
$$\text{implicit stages}\begin{cases} u^{n+\frac{11}{12}} - u^{n+1} &= -\frac{\Delta t}{12}u_t^{n+1} \\ u^{n+\frac{4}{5}} - u^{n+1} &= -\frac{\Delta t}{5}u_t^{n+\frac{11}{12}} \\ u^{n+1} &= \frac{\Delta t}{2}u_t^{n+\frac{4}{5}} + u^{n+\frac{1}{2}} \end{cases} \tag{28}$$

The weak forms associated with the explicit stages of the multi-stage $R_{3,3}$ scheme are as follows

$$\begin{aligned} (u^{n+\frac{1}{12}},\varphi) &= (u^n,\varphi) + \tfrac{\Delta t}{12}[(f^n,\varphi) - a(u^n,\varphi)] \\ (u^{n+\frac{1}{5}},\varphi) &= (u^n,\varphi) + \tfrac{\Delta t}{5}[(f^{n+\frac{1}{12}},\varphi) - a(u^{n+\frac{1}{12}},\varphi)] \\ (u^{n+\frac{1}{2}},\varphi) &= (u^n,\varphi) + \tfrac{\Delta t}{2}[(f^{n+\frac{1}{5}},\varphi) - a(u^{n+\frac{1}{5}},\varphi)] \end{aligned} \tag{29}$$

As before, we associate incremental unknowns with the implicit stages. Here, they are defined by

$$\boldsymbol{\Delta U} = \begin{Bmatrix} \Delta u^{n+\frac{4}{5}} \\ \Delta u^{n+\frac{11}{12}} \\ \Delta u^{n+1} \end{Bmatrix} = \begin{Bmatrix} u^{n+\frac{4}{5}} - u^{n+\frac{1}{2}} \\ u^{n+\frac{11}{12}} - u^{n+\frac{4}{5}} \\ u^{n+1} - u^{n+\frac{11}{12}} \end{Bmatrix}. \tag{30}$$

In this manner, the implicit stages can be written as in Eq.(19) with

$$\begin{aligned} \mathbf{A} &= \begin{bmatrix} \frac{3}{10} & -\frac{1}{5} & 0 \\ \frac{7}{60} & \frac{7}{60} & -\frac{1}{12} \\ \frac{1}{12} & \frac{1}{12} & \frac{1}{12} \end{bmatrix} \\ \boldsymbol{F} &= \Delta t \begin{Bmatrix} \frac{3}{10} \\ \frac{7}{60} \\ \frac{1}{12} \end{Bmatrix} \left(-\boldsymbol{a}\cdot\nabla\mathbf{u}^{\mathbf{n+\frac{1}{2}}} + \nu\nabla^{\mathbf{2}}\mathbf{u}^{\mathbf{n+\frac{1}{2}}} + \mathbf{f}^{\mathbf{n+\frac{1}{2}}}\right). \end{aligned} \tag{31}$$

Again, substituting the time derivatives by the original equation, Eq.(1), the weak form corresponding to the three implicit stages is Eq.(21) with

$$\boldsymbol{\Delta f} = \begin{Bmatrix} \Delta f^{n+\frac{4}{5}} \\ \Delta f^{n+\frac{11}{12}} \\ \Delta f^{n+1} \end{Bmatrix} = \begin{Bmatrix} f^{n+\frac{4}{5}} - f^{n+\frac{1}{2}} \\ f^{n+\frac{11}{12}} - f^{n+\frac{4}{5}} \\ f^{n+1} - f^{n+\frac{11}{12}} \end{Bmatrix} \tag{32}$$

and $\boldsymbol{\varphi} \in \left(\boldsymbol{H}_0^1(\Omega)\right)^3$. In this case, we can also find a more compact formulation of the multi-stage scheme using a generalization of Simpson's rule, it yields the following three-stage sixth-order method:

$$\begin{aligned}
\boldsymbol{\Delta U} &= \left\{ \begin{array}{c} \Delta u^{n+\alpha} \\ \Delta u^{n+\beta} \\ \Delta u^{n+1} \end{array} \right\} = \left\{ \begin{array}{c} u^{n+\alpha} - u^n \\ u^{n+\beta} - u^{n+\alpha} \\ u^{n+1} - u^{n+\beta} \end{array} \right\} \\
&= \frac{\Delta t}{120} \left[ \begin{array}{cccc} 11+\sqrt{5} & 25-\sqrt{5} & 25-13\sqrt{5} & \sqrt{5}-1 \\ -2\sqrt{5} & 14\sqrt{5} & 14\sqrt{5} & -2\sqrt{5} \\ \sqrt{5}-1 & 25-13\sqrt{5} & 25-\sqrt{5} & 11+\sqrt{5} \end{array} \right] \left\{ \begin{array}{c} u_t^n \\ u_t^{n+\alpha} \\ u_t^{n+\beta} \\ u_t^{n+1} \end{array} \right\}
\end{aligned} \tag{33}$$

where $\alpha = (5-\sqrt{5})/10$ and $\beta = (5+\sqrt{5})/10$. The weak form corresponding to this more compact multi-stage scheme is also determined by Eq.(21) with

$$\mathbf{A} = \frac{1}{120} \left[ \begin{array}{ccc} 49-13\sqrt{5} & 12(2-\sqrt{5}) & \sqrt{5}-1 \\ 26\sqrt{5} & 12\sqrt{5} & -2\sqrt{5} \\ 61-13\sqrt{5} & 36 & 11+\sqrt{5} \end{array} \right]$$

$$\boldsymbol{\Delta f} = \left\{ \begin{array}{c} \Delta f^{n+\alpha} \\ \Delta f^{n+\beta} \\ \Delta f^{n+1} \end{array} \right\} = \left\{ \begin{array}{c} f^{n+\alpha} - f^n \\ f^{n+\beta} - f^{n+\alpha} \\ f^{n+1} - f^{n+\beta} \end{array} \right\} \tag{34}$$

$$\boldsymbol{F} = \frac{\Delta t}{120} \left\{ \begin{array}{c} 12(5-\sqrt{5}) \\ 24\sqrt{5} \\ 12(5-\sqrt{5}) \end{array} \right\} \left(-\boldsymbol{a} \cdot \nabla \mathbf{u^n} + \nu \nabla^2 \mathbf{u^n} + \mathbf{f^n}\right).$$

**Remarks:**

1. When using the above high-order accurate implicit methods in combination with finite elements for spatial discretization, the dimension of the system of semidiscrete equations to be solved at each time step is, as we have seen, increased (doubled for the fourth-order method, tripled for the sixth-order one) with respect to traditional second order methods, such as the Crank-Nicolson scheme. This is unfortunately the price to pay to obtain methods which are simultaneously high order accurate and A-stable. However these high-order time schemes permit the use of larger time-step values for an identical global time accuracy.

2. When dealing with pure convection problems it is generally possible to express the second time derivative of the unknown in terms of spatial derivatives. It follows that multi-stage schemes incorporating both

first and second time derivatives can be employed for solving problems describing purely convective transport. In this respect, approximation $R_{2,2}$ can be used directly in pure convection problems, as shown in references 3, 4 where scheme (14) is used directly in combination with linear elements for spatial discretization.

3. If we admit second derivatives, the sixth-order approximation $R_{3,3}$ can also be specialized to deal with pure convection problems. The result of its factorization in the form

$$\left(1-\frac{x}{2}(1-\frac{x}{5}+\frac{x^2}{60})\right)u^{n+1} = \left(1+\frac{x}{2}(1+\frac{x}{5}+\frac{x^2}{60})\right)u^n \qquad (35)$$

is a four-stage method including two explicit phases and two implicit ones as follows:

$$\left\{\begin{array}{rcl} u^{n+\frac{1}{5}} &=& u^n + \frac{\Delta t}{5}u_t^n + \frac{\Delta t^2}{60}u_{tt}^n \\ u^{n+\frac{1}{2}} &=& u^n + \frac{\Delta t}{2}u_t^{n+\frac{1}{5}} \\ u^{n+\frac{4}{5}} &=& u^{n+1} - \frac{\Delta t}{5}u_t^{n+1} + \frac{\Delta t^2}{60}u_{tt}^{n+1} \\ u^{n+1} &=& u^{n+\frac{1}{2}} + \frac{\Delta t}{2}u_t^{n+\frac{4}{5}} \end{array}\right. \qquad (36)$$

## 2.3 Least-squares spatial discretization of implicit Padé schemes

So far, a conventional Galerkin formulation has been tacitly assumed for the spatial representation of the convection-diffusion equation. As is well known, this fails to produce stable results when convection dominates the transport process, especially when the Galerkin finite element method is combined with a non-dissipative time integration scheme, such as the $R_{n,n}$ Padé methods (see Section 3). A Petrov-Galerkin form of the method of weighted residuals should therefore be introduced to avoid unphysical oscillatory results in problems characterized by a high value of the Péclet number. In the present context of purely transient problems, a modified weighting of the residual of the convection-diffusion equation can be obtained using a least-squares approach, as first suggested by Carey and Jiang[21] for second order time-stepping schemes and subsequently generalized by Park and Liggett[22] for third and fourth order methods. The weighting function does not depend on any new adjustable parameter. In fact, the added diffusion depends on the time step employed in the integration scheme. In this Section, the above least-squares formulation is generalized to the case of an A-stable multi-stage Padé scheme.

### 2.3.1 Least-squares formulation of the Padé scheme

The strong form corresponding to Eq.(21) is given by Eq.(19) in which the time derivative is replaced with spatial derivatives. This gives

$$\boldsymbol{\mathcal{F}}(\boldsymbol{\Delta U}) = \boldsymbol{R} \tag{37}$$

where

$$\begin{aligned} \boldsymbol{\mathcal{F}}(\boldsymbol{\Delta U}) &= \left[\boldsymbol{I} + \Delta t\, \boldsymbol{A}\left(\boldsymbol{a}\cdot\nabla - \nu\nabla^{\mathbf{2}}\right)\right]\boldsymbol{\Delta U} \\ \boldsymbol{R} &= \Delta t\, \boldsymbol{A}\boldsymbol{\Delta f} + \boldsymbol{F} \end{aligned} \tag{38}$$

The least-squares problem associated with Eq.(37) is defined by

$$\boldsymbol{\mathcal{F}}^{*}\,\boldsymbol{\mathcal{F}}(\boldsymbol{\Delta U}) = \boldsymbol{\mathcal{F}}^{*}\,\boldsymbol{R} \tag{39}$$

where $\boldsymbol{\mathcal{F}}^{*}$ is the adjoint operator of $\boldsymbol{\mathcal{F}}$. The weak form corresponding to this relationship is given by

$$(\boldsymbol{\mathcal{F}}^{*}\boldsymbol{\mathcal{F}}(\boldsymbol{\Delta U}), \boldsymbol{\varphi}) = (\boldsymbol{\mathcal{F}}^{*}\boldsymbol{R}, \boldsymbol{\varphi})\,. \tag{40}$$

Furthermore, in view of the property of adjoint operators, Eq.(40) can be transformed to

$$(\boldsymbol{\mathcal{F}}(\boldsymbol{\Delta U})\,,\, \boldsymbol{\mathcal{F}}(\boldsymbol{\varphi})) = (\boldsymbol{R}, \boldsymbol{\mathcal{F}}(\boldsymbol{\varphi}))\,, \tag{41}$$

Now, replacing in this relationship operators $\boldsymbol{\mathcal{F}}$ and $\boldsymbol{R}$ from their definition in Eq.(38) yields the following expression for the weak form associated with the least-squares formulation of the multi-stage implicit Padé problem:

$$\begin{aligned} &(\boldsymbol{\Delta U} + \Delta t\, \boldsymbol{A}\left[\boldsymbol{a}\cdot\nabla\boldsymbol{\Delta U} - \nu\nabla^{\mathbf{2}}\boldsymbol{\Delta U}\right]\,,\, \boldsymbol{\varphi} + \Delta t\, \boldsymbol{A}\left[\boldsymbol{a}\cdot\nabla\boldsymbol{\varphi} - \nu\nabla^{\mathbf{2}}\boldsymbol{\varphi}\right]) \\ =\;& (\boldsymbol{F} + \Delta t\, \boldsymbol{A}\,\boldsymbol{\Delta f}\,,\, \boldsymbol{\varphi} + \Delta t\, \boldsymbol{A}\left[\boldsymbol{a}\cdot\nabla\boldsymbol{\varphi} - \nu\nabla^{\mathbf{2}}\boldsymbol{\varphi}\right]) \end{aligned} \tag{42}$$

At this point it is clearly apparent that the Padé-Least squares formulation naturally introduces modified weighting functions that possess the same tensorial structure as the SUPG and Galerkin/Least-squares weighting functions, but without any adjustable parameter (apart from the usual ones: $\Delta t$ and $h$) in the linear combination of the standard Galerkin weighting function and the added functions.

As with other Petrov-Galerkin formulations, the added terms to the standard Galerkin weighting function are assumed to only affect the element interiors and Eq.(41) is, therefore, rewritten in the form

$$\begin{aligned} (\boldsymbol{\mathcal{F}}(\boldsymbol{\Delta U}), \boldsymbol{\varphi}) &+ \Delta t \sum_{e} \int_{\Omega_e} \boldsymbol{\mathcal{F}}(\boldsymbol{\Delta U}) \cdot \boldsymbol{A}\left[\boldsymbol{a}\cdot\nabla\boldsymbol{\varphi} - \nu\nabla^{\mathbf{2}}\boldsymbol{\varphi}\right] d\Omega = \\ (\boldsymbol{R},\, \boldsymbol{\varphi}) &+ \Delta t \sum_{e} \int_{\Omega_e} \boldsymbol{R} \cdot \boldsymbol{A}\left[\boldsymbol{a}\cdot\nabla\boldsymbol{\varphi} - \nu\nabla^{\mathbf{2}}\boldsymbol{\varphi}\right] d\Omega, \end{aligned} \tag{43}$$

with index $e$ ranging from 1 to the number of elements in the finite element discretization of $\Omega$. For rectangular bilinear elements in 2D or trilinear elements in 3D, one has that $\nabla^2\boldsymbol{\varphi} \equiv 0$ within each element. This is also the cases with linear triangles and tetrahedra. However, this term cannot be neglected if higher-order elements are used. It is important to notice that the previous equation is obviously consistent with the high-order time integration schemes developed. It differs from the standard Galerkin one by terms proportional to $\Delta t$. Namely,

$$\Delta t \sum_e \int_{\Omega_e} [\boldsymbol{\mathcal{F}}(\boldsymbol{\Delta U}) - \boldsymbol{R}] \cdot \boldsymbol{A} \left[ \boldsymbol{a} \cdot \nabla \boldsymbol{\varphi} - \nu \nabla^2 \boldsymbol{\varphi} \right] d\Omega.$$

This term, however, is of order $\Delta t^{n+m+1}$, where $m$ and $n$ characterize the Padé approximation $R_{n,m}$, because Eq.(37) is already discretized in time and thus of order $n+m$.

# 3 Properties of Padé approximations

## 3.1 Stability analysis

The spatial discretization of the convection-diffusion equation using finite elements leads to the following system of differential equations to be solved at each station of the time integration procedure:

$$\frac{d\mathbf{u}}{dt} = \mathbf{R}(\mathbf{u}) \tag{44}$$

where $\mathbf{u}$ is the vector collecting the nodal values of the unknown and $\mathbf{R}(\mathbf{u})$ stands for the nodal loads arising from the discretization of the first- and second-order spatial operators.

In order to discuss the stability of any time-integration method applied to Eq.(44), we first define the eigenvalues $\lambda$ of the spatial discretization operator $\mathbf{R}$ as

$$\mathbf{R}(\mathbf{v}) = \lambda \mathbf{v} \tag{45}$$

where $\mathbf{v}$ is the eigenvector associated to the eigenvalue $\lambda$.

If $\mathbf{R}(\mathbf{u})$ corresponds to the spatially discrete form of a diffusion operator, the eigenvalues are purely real and negative. On the other hand, if $\mathbf{R}(\mathbf{u})$ arises from the discretization of a convection operator, its eigenvalues are complex with a negative real part if upwind approximations are employed, whereas the real part is zero and the eigenvalues are purely imaginary whenever a central spatial approximation (e.g., the Galerkin projection) is used.

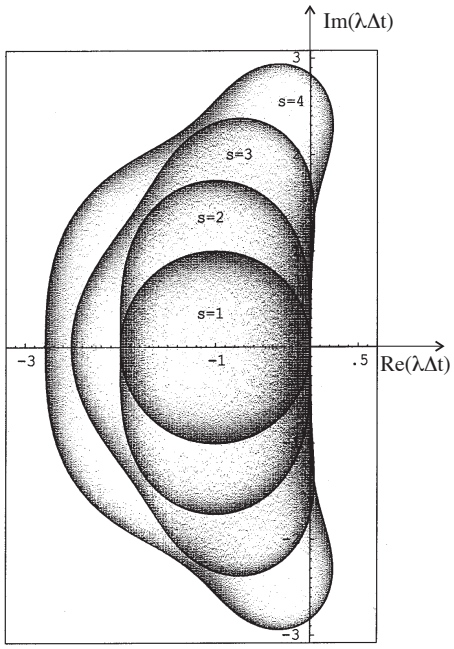


Figure 1: Stability domain of explicit Padé and Runge-Kutta methods of order $s$.

The stability of the method is ensured if and only if the time step is such that the value of the modulus of the amplification factor $G = u^{n+1}/u^n$ is less than unity for all the eigenvalues of the discretization operator $\mathbf{R}$. By definition, the amplification factor $G$ of a Padé approximation $R_{n,m}$ has the same structure as the approximation itself:

$$G_{n,m} = R_{n,m}(\lambda \Delta t). \tag{46}$$

It follows that Table 1 contains the amplification factors of all Padé approximations considered herein, provided we pose $x = \lambda \Delta t$.

In situations where diffusive effects are small with respect to the convective ones, the eigenvalues of $\mathbf{R}$ are distributed close to the imaginary axis of the $\lambda \Delta t$ complex plane. A time integration method whose stability region encloses part of the imaginary axis is then necessary.

In the frame of explicit methods, the forward Euler first-order scheme, the stability region of which does not enclose any portion of the imaginary axis of the $\lambda \Delta t$ complex plane, has therefore to be rejected in favor, for instance, of higher-order explicit Padé approximations or Runge-Kutta methods. As shown in Figure 1 from reference 11, explicit methods of higher order do enclose a portion of the imaginary axis. For example, the fourth-order explicit Padé method and the equivalent classical fourth-order Runge-Kutta method

cut the imaginary axis at $\pm 2\sqrt{2}$ (see Figure 1) and since their absolute stability region contains a finite portion of the imaginary axis of the $\lambda \Delta t$ plane, the methods can be used in convection dominated situations. However, even if an explicit method has a stability domain which encloses part of the imaginary axis, the problem of a maximum allowable time step still remains. This is actually the case for all explicit methods.

We have to turn to implicit methods in order to reach unconditional stability. The stability domain then encloses the whole left half-plane of the $\lambda \Delta t$ complex plane, including the imaginary axis. Some implicit Padé approximations do possess the interesting property of unconditional stability or A-stability. As shown in references 10, 12, a Padé approximation $R_{n,m}$ is unconditionally stable if it satisfies the condition:

$$m - 2 \leq n \leq m \Longleftrightarrow R_{n,m} \text{ is A-stable} \tag{47}$$

It follows that the implicit Padé approximations

$$R_{0,1},\ R_{1,1},\ R_{0,2},\ R_{1,2},\ R_{2,2},\ R_{1,3},\ R_{2,3},\ R_{3,3}$$

are A-stable and therefore potentially interesting for the time integration of convection-diffusion equations.

Note that these results do no contradict the second Dahlquist barrier theorem[12] because the previous cited implicit Padé approximations for orders 3 or higher are not linear multistep techniques. They have several implicit stages.

## 3.2 Phase and damping responses

The accuracy properties of explicit Padé schemes have been discussed elsewhere (see for instance references 3 and 4) and will not be considered any further herein. We shall instead concentrate on the phase and damping responses of the implicit multi-stage Padé schemes.

To analyze the accuracy properties of such implicit schemes, we consider their application to the linear convection-diffusion equation

$$\frac{\partial u}{\partial t} + a \frac{\partial u}{\partial x} = \nu \frac{\partial^2 u}{\partial x^2}, \tag{48}$$

using a uniform mesh of linear elements of size $h$. We then substitute a Fourier mode $e^{ikx}$ into the resulting discrete scheme and, defining the dimensionless wave number $\xi = k\,h$, obtain the eigenvalues of the spatial discretization operator in the form

$$\lambda = \frac{1}{\Delta t}\, g(\xi\,,\, c\,,\, d). \tag{49}$$

Here, $c = a\Delta t/h$ is the Courant number and $d = \nu\,\Delta t/h^2$ the diffusion number. The amplification factor $G_{n,m}$ corresponding to Padé scheme $R_{n,m}$ is then given by

$$G_{n,m} = R_{n,m}(g(\xi, c, d)) \tag{50}$$

The corresponding quantity for the partial differential equation (48) is

$$G_{exact} = \mathrm{e}^{-(\delta + i\omega)} \tag{51}$$

where $\delta = d\xi^2$ and $\omega = c\xi$ are the exact damping and the exact frequency, respectively. To evaluate the accuracy of the Padé schemes beyond the asymptotic limit $\Delta t \to 0$, we introduce the damping $\delta_{num}$ and frequency $\omega_{num}$ of the fully discrete schemes through the relation

$$G_{n,m} = \mathrm{e}^{-(\delta_{num} + i\omega_{num})} \tag{52}$$

which implies

$$\begin{aligned} \delta_{num} &= -\ln|G_{n,m}| \\ \omega_{num} &= \arg(G_{n,m})\,. \end{aligned} \tag{53}$$

On this basis, the frequency response of the schemes can be characterized by the relative phase error $\Delta = \omega_{num}/\omega - 1$, and their damping response by the damping ratio $\delta_{num}/\delta$.

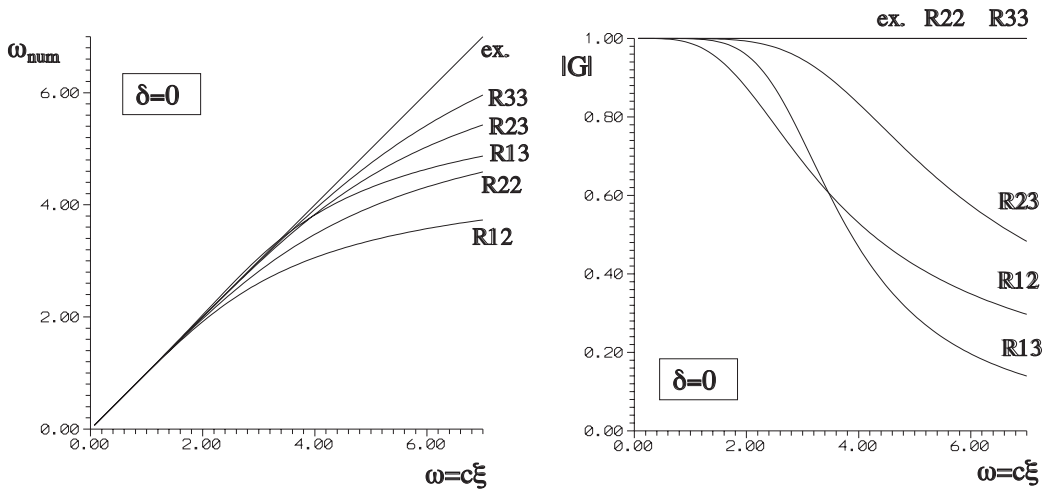


Figure 2: Accuracy of some A-stable Padé approximations for pure convection.

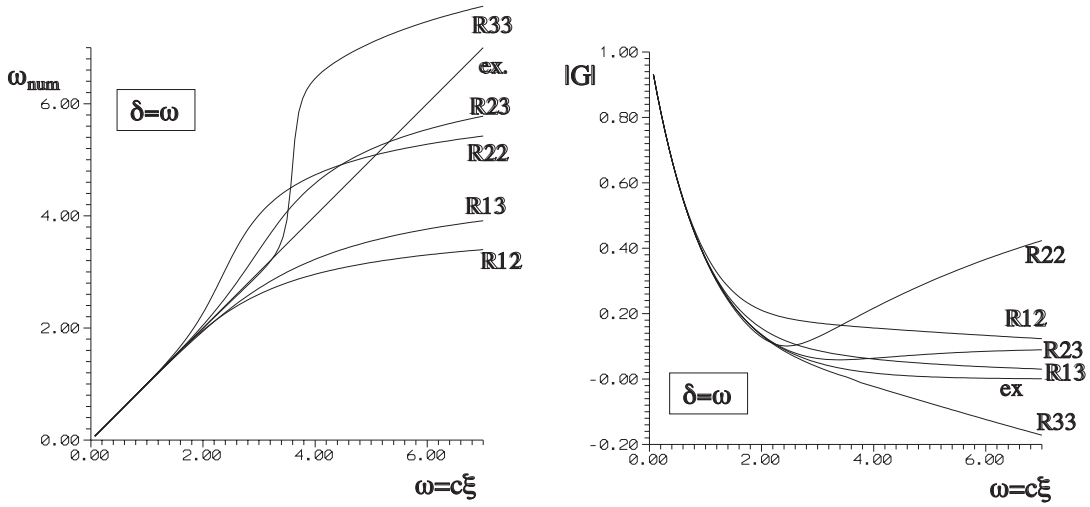


Figure 3: Accuracy of some A-stable Padé approximations for convection-diffusion.

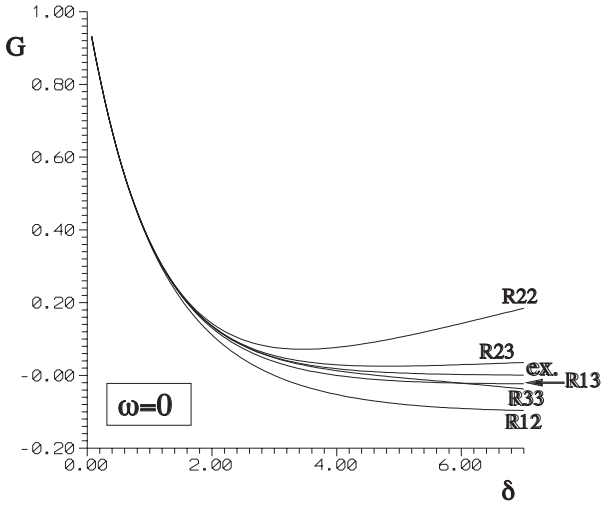


Figure 4: Accuracy of some A-stable Padé approximations for pure diffusion.

Figures 2 to 4 give a graphical representation of the phase and damping responses of selected implicit Padé schemes. Recall that the amplification factor of the schemes is given by the simple relationship (50).

In the case of pure convection (Figure 2), we note that, as expected, the frequency response improves with the temporal accuracy of the multi-stage Padé schemes. We also observe that, for each scheme, there is clearly an accuracy limit. In practice, this means that there is an upper value of the Courant number beyond which there is a progressive degradation in the

phase accuracy. We also note from Figure 2 that the off-diagonal approximants yield dissipative schemes, while the $R_{n,n}$ schemes are non-dissipative. As a consequence, such schemes are not ideally suited to deal with pure convection problems if centered (Galerkin) approximations are used for spatial discretization. These methods should therefore be combined with Petrov-Galerkin methods (such as the SUPG,[18] the Galerkin-Least-squares,[19] the Taylor-Least squares[21,22] , or the present Padé-Least-squares methods) for the spatial representation.

Figure 3 illustrates the frequency and damping responses for a mixed convective-diffusive situation characterized by $\delta = \omega$. We see that all schemes exhibit a very good phase accuracy up to $\omega \simeq 2$ and that there is a systematic accuracy degradation beyond this value. The same applies to the damping response, with all schemes being under-diffusive at elevated frequencies, except $R_{3,3}$ which is over-diffusive.

Finally, for the case of purely diffusive transport, Figure 4 indicates an accurate response of all schemes up to $\delta = d\xi^2 \simeq 2$. This means that, in the range of accurate resolution ($0 \leq \xi \leq \pi/4$), all schemes can be safely operated with a value of the diffusion number $d$ of the order of 3. One also notes that approximants $R_{1,3}$ and $R_{3,3}$ are the most accurate in pure diffusion with an excellent response up to about $\delta = 6$.

# 4 Similarities between Padé and Runge-Kutta methods

The Runge-Kutta methods are multi-stage methods that only make use of the solution $u^n$ at time $t^n$ to compute the next solution $u^{n+1}$. This is achieved by computing a number $k$ of intermediate values of the time derivative of the unknown $u$, within the interval $\Delta t = t^{n+1} - t^n$. Applied to the differential equation

$$\frac{du}{dt} = R(u,t) \tag{54}$$

the most general form of a $k$-stage Runge-Kutta method is written as follows:[10–12]

$$\delta_i = \Delta t\, R\left( u^n + \sum_{j=1}^{k} a_{ij}\, \delta_j\, ,\, t^n + c_i \Delta t \right) \qquad i = 1, \ldots, k \tag{55}$$

$$u^{n+1} = u^n + \sum_{i=1}^{k} b_i\, \delta_i \tag{56}$$

The associated consistency conditions are[10–12]

$$c_i = \sum_{j=1}^{k} a_{ij} \qquad \text{and} \qquad \sum_{i=1}^{k} b_i = 1 \tag{57}$$

The widely used explicit Runge-Kutta methods are such that $a_{ij} = 0$ for $j \geq i$. If this condition is not satisfied, the methods are implicit.

In the explicit algorithms of order $n$, like the $R_{n,0}$ Padé approximants or the explicit Runge-Kutta methods, the amplification factor $G(z)$, where $z = \lambda \Delta t$ (see Eq.(46)), is given by the polynomial

$$G(z) = 1 + \frac{z}{1!} + \frac{z^2}{2!} + \cdots + \frac{z^n}{n!} + T(z) \tag{58}$$

where $T(z) = O(z^{n+1})$. That is,

$$G(z) = R_{n,0}(z) + T(z) \tag{59}$$

The polynomial structure of $G(z)$ in equation (58) indicates why explicit methods cannot be A-stable. In the multi-stage explicit Padé methods, one has $T(z) = 0$ and the same holds for the explicit $n$-stage Runge-Kutta methods of order $n$.[10] Thus, the multi-stage explicit Padé schemes and the $n$-stage Runge-Kutta methods of order $n$ are equivalent in application to linear problems. The only difference resides in the numerical implementation of the methods. Recall that the maximum order of a $n$-stage $n$-order explicit Runge-Kutta method is 4.

Among the implicit methods, $k$-stage Runge-Kutta methods of order $2k$ are called the Gauss methods. There are other classical families of implicit Runge-Kutta methods, such as the Radau-IA and Radau-IIA $k$-stage methods of order $2k-1$, and the Lobatto-IIIA, Lobatto-IIIB and Lobatto IIIC $k$-stage methods of order $2k-2$.[10–12] As indicated in Table 2 from reference 12, the various families of Runge-Kutta methods mentioned above are intimately related to the Padé multi-stage methods in the sense that they possess identical amplification factors.

Another family of implicit Runge-Kutta methods includes the so-called diagonally implicit (DIRK) methods. The great advantage of such methods is the absence of coupling between the various stages ($a_{ij} = 0$ in Eq.(55) for $i < j$), which reduces the size of the systems to be solved at each step of the time integration procedure. Unfortunately, the accuracy properties of the DIRK methods in mixed convection-diffusion situations are significantly inferior to those of the classical implicit Runge-Kutta methods and of the implicit Padé schemes.[9,11]

| Implicit RK method | multi-stage Padé method | Order | Amplification factor |
|---|---|---|---|
| Gauss | $R_{n,n}$ | $2n$ | $R_{n,n}(z)$ |
| Radau IA | $R_{n-1,n}$ | $2n-1$ | $R_{n-1,n}(z)$ |
| Radau IIA | $R_{n-1,n}$ | $2n-1$ | $R_{n-1,n}(z)$ |
| Lobatto IIIA | $R_{n-1,n-1}$ | $2n-2$ | $R_{n-1,n-1}(z)$ |
| Lobatto IIIB | $R_{n-1,n-1}$ | $2n-2$ | $R_{n-1,n-1}(z)$ |
| Lobatto IIIC | $R_{n-2,n}$ | $2n-2$ | $R_{n-2,n}(z)$ |

Table 2: Relationship between implicit Runge-Kutta methods and multi-stage Padé schemes.

# 5 Numerical examples

Numerical tests were performed to assess the performance of selected implicit Padé schemes of high order in the solution of convection and convection-diffusion problems. The selected schemes are $R_{1,2}$, $R_{2,2}$, $R_{2,3}$ and $R_{3,3}$.

## 5.1 Convection-Diffusion of a Gaussian Profile

To illustrate the performance of the selected high-order Padé schemes and compare them to standard explicit schemes, consider first the linear convection-diffusion problem over the spatial interval $[0, 150]$ defined by the following initial and boundary conditions:

$$\begin{aligned} u(x,0) &= \frac{2.5}{\sigma} e^{-\frac{1}{2}X^2} \\ u(0,t) &= 0 \\ u(150,t) &= \frac{2.5}{\sigma_1} e^{-\frac{1}{2}L^2} \end{aligned} \tag{60}$$

with $X = (x - x_0)/\sigma$, $\sigma = 3.5$, $L = (150 - x_0 - t)/\sigma_1$, $\sigma_1 = \sigma\sqrt{1 + 2\nu t/\sigma^2}$ and $x_0 = 20$ for $Pe = 5$ and $x_0 = 60$ for $Pe = 0.1$. A unit convection velocity is assumed and the calculations were made using a uniform mesh of linear elements with $h = 1$.

In Figures 5 to 10, we compare the profiles of the Gaussian obtained at various time levels with the implicit Padé schemes $R_{1,2}$, $R_{2,2}$, $R_{2,3}$ and $R_{3,3}$ with the three-stage explicit scheme $R_{3,0}$ (3TG) and with the second order explicit scheme of Peraire[20] (TG2Pe). Two values of the Péclet number were considered, namely $Pe = 0.1$ and $Pe = 5$. The results for $Pe = 0.1$ are at times $t = 0$, 2, 6, 24, while they are at times $t = 0$, 12, 60, 108 for $Pe = 5$.

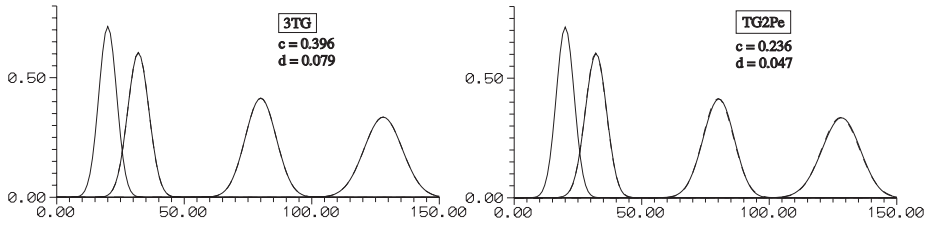


Figure 5: Convection-diffusion of a Gaussian by 3TG[15] and TG2Pe[20] with $Pe = 5$ for $t = 0$, 12, 60, 108.

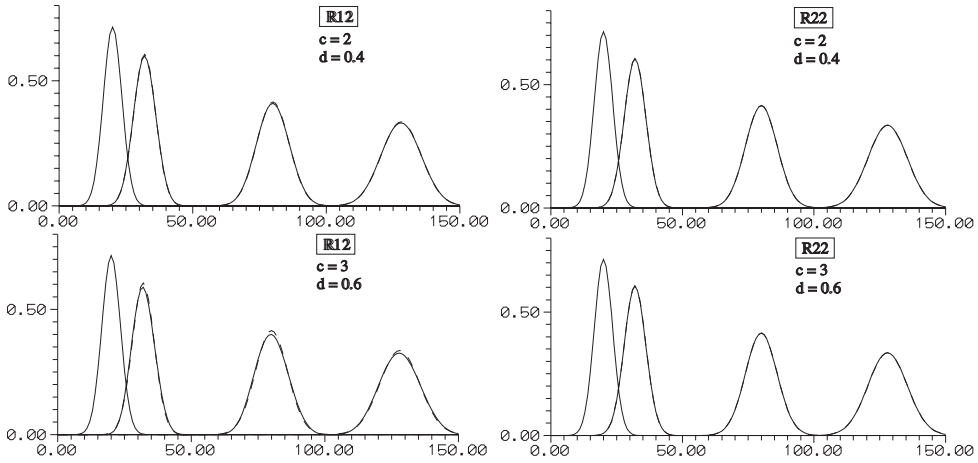


Figure 6: Convection-diffusion of a Gaussian by $R_{1,2}$ and $R_{2,2}$ with $Pe = 5$ at $c = 2$, 3 for $t = 0$, 12, 60, 108.

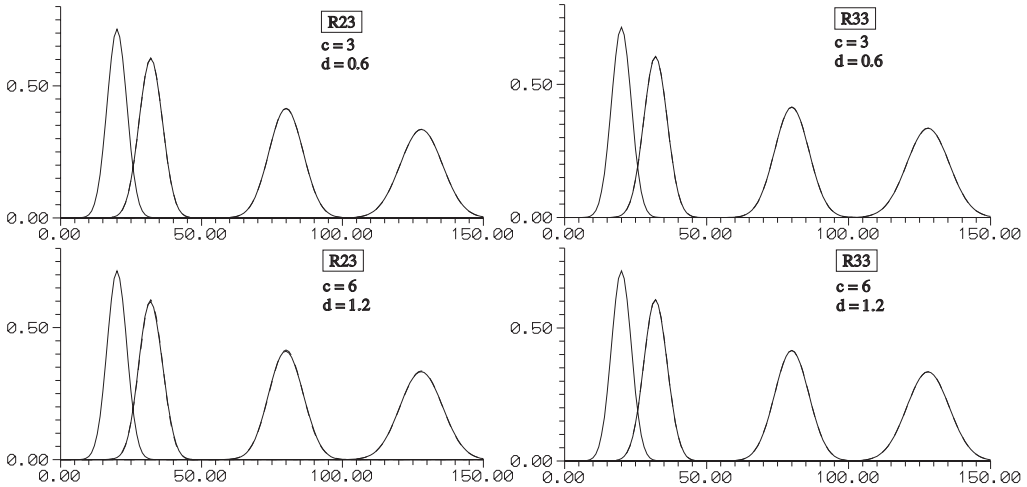


Figure 7: Convection-diffusion of a Gaussian by $R_{2,3}$ and $R_{3,3}$ with $Pe = 5$ at $c = 3$, 6 for $t = 0$, 12, 60, 108.

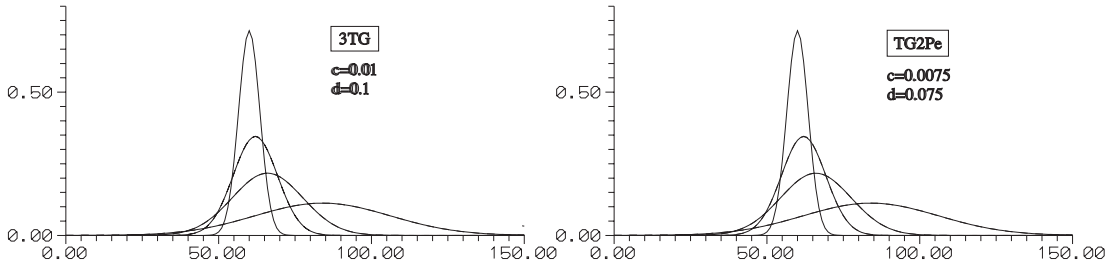


Figure 8: Convection-diffusion of a Gaussian by 3TG[15] and TG2Pe[20] with $Pe = 0.1$ for $t = 0$, 2, 6, 24.

The explicit schemes were operated with a time step equal to 90 percent of their critical value, while the implicit ones used large values of the Courant number $c$ to appraise their accuracy well beyond the stability limit of the explicit schemes. The results indicate that the implicit schemes can produce very accurate answers for large values of the time step. The discontinuous lines in Figures 5 to 10 correspond to the analytical solution of the problem.

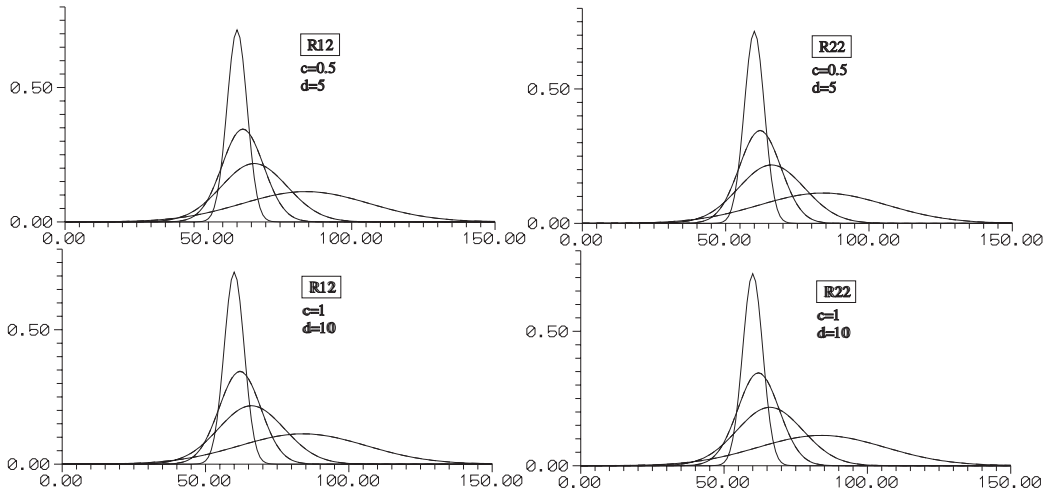


Figure 9: Convection-diffusion of a Gaussian by $R_{1,2}$ and $R_{2,2}$ with $Pe = 0.1$ at $c = 0.5$, 1 for $t = 0$, 2, 6, 24.

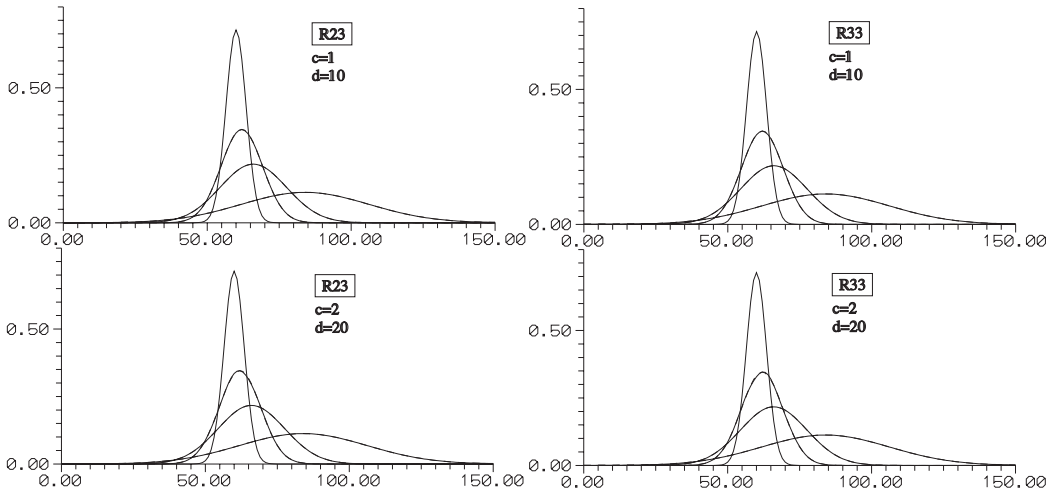


Figure 10: Convection-diffusion of a Gaussian by $R_{2,3}$ and $R_{3,3}$ with $Pe = 0.1$ at $c = 1$, 2 for $t = 0$, 2, 6, 24.

## 5.2 Rotating Cosine Hill

This standard test problem considers the convection of a product cosine hill in a 2D pure rotation velocity field. The initial conditions are

$$u(\mathbf{x}, 0) = \begin{cases} \frac{1}{4}\left[1 + \cos \pi X_1\right]\left[1 + \cos \pi X_2\right] & \text{if } X_1^2 + X_2^2 \leq 1 \\ 0 & \text{otherwise} \end{cases}$$

where $\mathbf{X} = (\mathbf{x} - \mathbf{x}_0)/\sigma$, $\mathbf{x}_0$ and $\sigma$ being the initial position of the center and the radius of the cosine hill. The advection field is a pure rotation with unit angular velocity given by $\boldsymbol{a}(\mathbf{x}) = (-x_2, x_1)$

A uniform mesh of $30 \times 30$ quadrilateral elements over the unit square $[-\frac{1}{2}, \frac{1}{2}] \times [-\frac{1}{2}, \frac{1}{2}]$ has been employed in the calculations and the standard Galerkin finite element method has been used for the spatial discretization.

Here again, the implicit methods $R_{1,2}$, $R_{2,2}$, $R_{2,3}$ and $R_{3,3}$ are compared to the explicit schemes $3TG$ and $TG2Pe$. The numerical solutions for the case $\mathbf{x}_0 = (\frac{1}{6}, \frac{1}{6})$ and $\sigma = 0.2$ are shown in Figures 11 and 12. They give the elevations of the rotating cosine hill after one full revolution. To compare the accuracy of the various schemes, the maximum and minimum values of the computed solutions are provided, together with the value of the maximum Courant number in the finite element mesh. One notes that by contrast with the explicit schemes the implicit methods can be accurately operated with quite large time steps. Scheme $R_{1,2}$ appears to be the less accurate implicit A-stable method as could be expected from the accuracy properties shown in Figures 2-4.

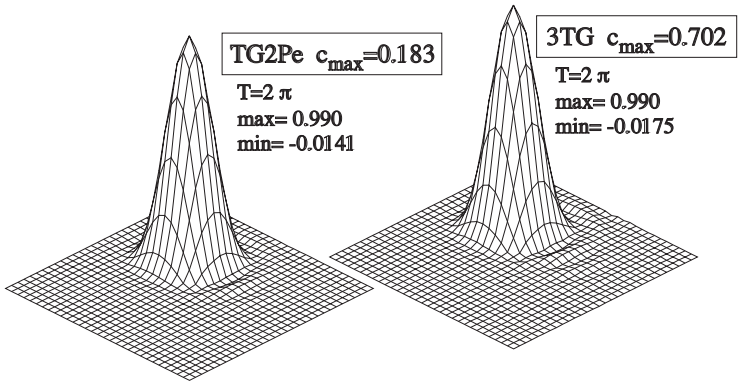


Figure 11: Solution of the Rotating Cosine Hill using $3TG$ and $TG2Pe$ explicit methods.

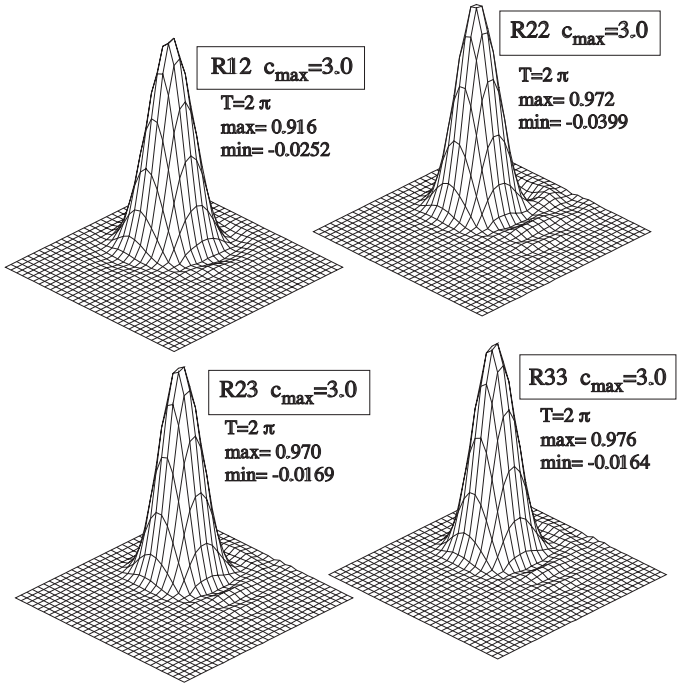


Figure 12: Solution of the Rotating Cosine Hill with the implicit Padé schemes $R_{1,2}$, $R_{2,2}$, $R_{2,3}$ and $R_{3,3}$ for $c = 3$.

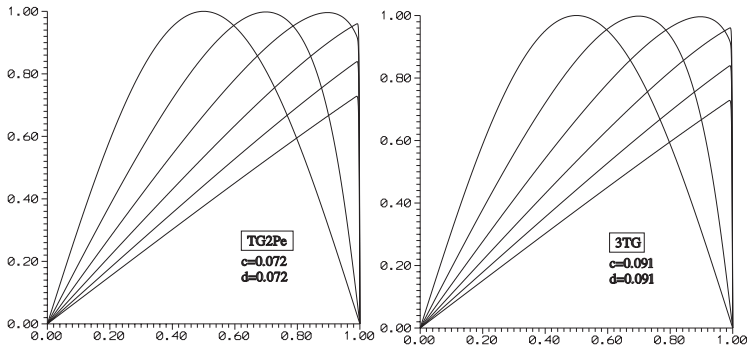


Figure 13: Solution of 1D Burgers equation by 3TG[15] and TG2Pe[20] with $Pe = 1$ for $t = 0$, 0.2, 0.4, 0.6, 0.8, 1.0.

## 5.3 Burgers equation in 1D

One of the main objectives of the A-stable implicit methods is to solve nonlinear stiff problems. As a first nonlinear test, we have solved the Burgers advection-diffusion equation in 1D to appraise the performance of the high-order Padé schemes with respect to the standard explicit schemes. We consider the Burgers problem over the spatial interval $[0, 1]$ defined by

$$\begin{aligned} u_t + uu_x &= \nu u_{xx} \\ u(x,0) &= \sin(\pi x) \\ u(0,t) &= u(1,t) = 0 \end{aligned} \tag{61}$$

for $Pe = 1$ and $\nu = 0.001$. A uniform mesh of linear elements of size $h = 0.001$ has been used.

Figures 13 to 14 show the results obtained with both implicit and explicit methods and one can appreciate the efficiency of the high order Padé methods from the test data in Table 3. The $R_{2,3}$ and the $R_{3,3}$ methods are more than seven times faster than the TG2Pe method, and more than seventeen times faster than the 3TG method. The explicit schemes were operated with a time step equal to 75 percent of their critical value, while $R_{2,3}$ and $R_{3,3}$ used large values of the Courant number $c$. Note that in the $R_{2,3}$ and $R_{3,3}$ methods a nonlinear system had to be solved at each time station by Newton-Raphson iteration. Only two iterations were needed to obtain an accuracy in excess of $10^{-4}$.

This simple test problem provides a good illustration of the penalization introduced by the conditional stability of explicit methods when a refined spatial discretization of convection–diffusion problems is required.

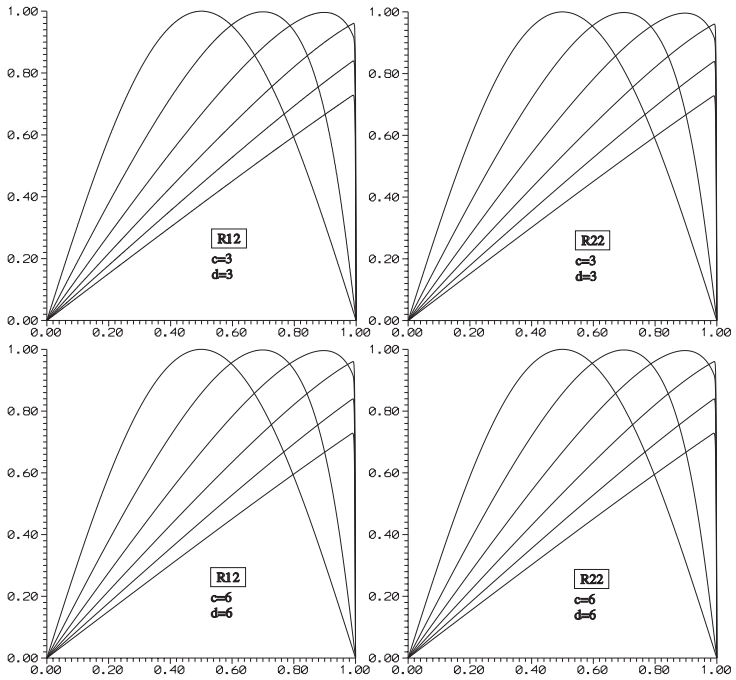


Figure 14: Solution of 1D Burgers equation by $R_{1,2}$ and $R_{2,2}$ with $Pe = 1$ at $c = 3$, 6 for $t = 0$, 0.2, 0.4, 0.6, 0.8, 1.0.

| method | $c_{max}$ | $d$ | $\Delta t$ | CPU | Time steps |
|---|---|---|---|---|---|
| TG2Pe | 0.072 | 0.072 | 0.000072 | 2215 | 13809 |
| 3TG | 0.0907 | 0.0907 | 0.0000907 | 5216 | 10998 |
| R12 | 3 | 3 | 0.003 | 237 | 335 |
| R12 | 6 | 6 | 0.006 | 126 | 170 |
| R22 | 3 | 3 | 0.003 | 263 | 335 |
| R22 | 6 | 6 | 0.006 | 141 | 170 |
| R23 | 3 | 3 | 0.003 | 537 | 335 |
| R23 | 6 | 6 | 0.006 | 280 | 170 |
| R33 | 3 | 3 | 0.003 | 572 | 335 |
| R33 | 6 | 6 | 0.006 | 306 | 170 |

Table 3: Comparison of implicit Padé schemes and explicit methods for the 1D Burgers problem.

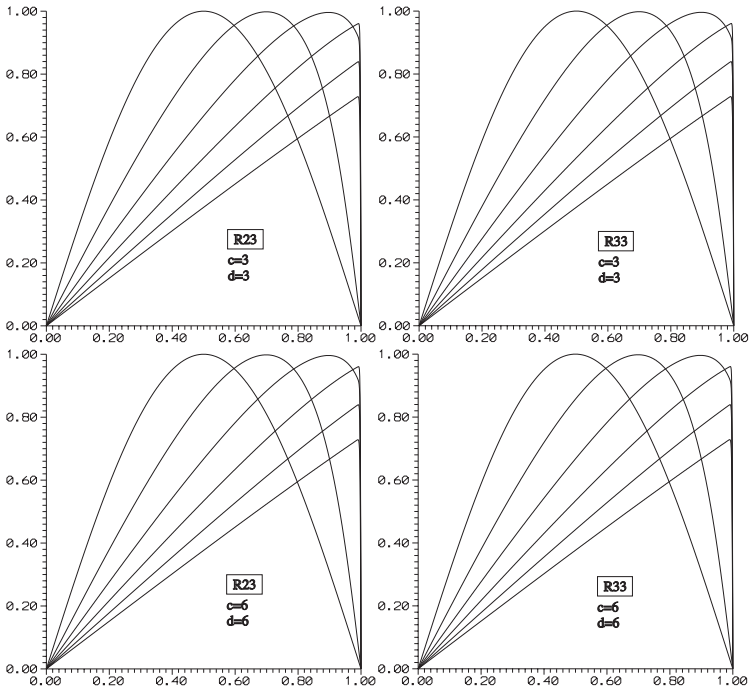


Figure 15: Solution of 1D Burgers equation by $R_{2,3}$ and $R_{3,3}$ with $Pe = 1$ at $c = 3$, 6 for $t = 0$, 0.2, 0.4, 0.6, 0.8, 1.0.

## 5.4 Nonlinear convection-diffusion problem in 2D

As a last test case, we consider the solution of a 2D Burgers problem over the square domain $\Omega = [0, 1] \times [0, 1]$ for which an analytical solution can be devised, thus allowing a direct assessment of the quality of the numerical results obtained with the high-order Padé schemes.

The problem is defined by the equations

$$\begin{aligned} u_t + (u, v) \cdot \nabla \mathbf{u} &= \nu \nabla^2 u \\ v_t + (u, v) \cdot \nabla \mathbf{v} &= \nu \nabla^2 v, \end{aligned} \tag{62}$$

which are coupled through their nonlinear convective terms, and by the following initial and boundary conditions:

$$\begin{aligned} &u(x, y, 0) = \sin(\pi x) \cos(\pi y) && v(x, y, 0) = \cos(\pi x) \sin(\pi y) \\ &u(0, y, t) = u(1, y, t) = 0 && v(x, 0, t) = v(x, 1, t) = 0 \\ &\frac{\partial u}{\partial n}(x, 0, t) = \frac{\partial u}{\partial n}(x, 1, t) = 0 && \frac{\partial v}{\partial n}(0, y, t) = \frac{\partial v}{\partial n}(1, y, t) = 0 \end{aligned} \tag{63}$$

The analytical solution to the above Burgers problem is given by

$$\begin{aligned} u(x,y,t) &= -2\nu\frac{\Phi_x(x,y,t)}{\Phi(x,y,t)} \\ v(x,y,t) &= -2\nu\frac{\Phi_y(x,y,t)}{\Phi(x,y,t)} \end{aligned} \tag{64}$$

where

$$\begin{aligned} \Phi(x,y,t) &= \textstyle\sum_{n,m=0}^{\infty} a_{nm}\cos(n\pi x)\cos(m\pi y)e^{-(n^2+m^2)\nu\pi^2 t} \\ \Phi_x(x,y,t) &= -\pi\textstyle\sum_{n=1,m=0}^{\infty} a_{nm} n\sin(n\pi x)\cos(m\pi y)e^{-(n^2+m^2)\nu\pi^2 t} \\ \Phi_y(x,y,t) &= -\pi\textstyle\sum_{n=0,m=1}^{\infty} a_{nm} m\cos(n\pi x)\sin(m\pi y)e^{-(n^2+m^2)\nu\pi^2 t} \end{aligned} \tag{65}$$

and $a_{nm}$ are the coefficients of a double Fourier series defined by

$$\begin{aligned} a_{00} &= \textstyle\int_0^1\int_0^1 e^{\cos(\pi x)\cos(\pi y)/(2\nu\pi)}\,dx\,dy \\ a_{n0}=a_{0n} &= 2\textstyle\int_0^1\int_0^1 e^{\cos(\pi x)\cos(\pi y)/(2\nu\pi)}\cos(n\pi x)\,dx\,dy \\ a_{nm}=a_{mn} &= 4\textstyle\int_0^1\int_0^1 e^{\cos(\pi x)\cos(\pi y)/(2\nu\pi)}\cos(n\pi x)\cos(m\pi y)\,dx\,dy. \end{aligned} \tag{66}$$

The problem defined by Eqs.(62) and (63) exhibits various symmetries. For instance, along a transverse section of the domain one has $u(x,x,t) = v(x,x,t)$ and $u(x,x,t) = -u(1-x,1-x,t)$. Moreover, one has $u(x,y,t) = v(y,x,t)$ and $u(x,y,t) = -u(1-x,1-y,t)$ over the global domain.

When convection dominates the nonlinear transport, the solution includes the formation of a shock along the diagonal of the domain passing through the points $(0,1)$ and $(1,0)$. Since a conventional Galerkin method is used herein for the spatial representation, the numerical solutions were computed for a moderate value of the Péclet number in order to avoid unphysical oscillations.

This 2D nonlinear problem is used to confirm the accuracy of the previously decribed Padé schemes. The knowledge of the analytical solution allows us to evaluate the maximum error norm over the space and time domain (namely, $\Omega\times[0,\,1]$). Figure 16 shows the convergence for $R_{1,2}$, $R_{2,2}$, $R_{2,3}$ and $R_{3,3}$ as $\Delta t$ decreases. Note that, as expected, the high-order accurate time-stepping schemes studied in the present figure exhibit the theoretical order of convergence.

The results obtained on a uniform mesh of $30\times 30$ bilinear elements with both explicit and implicit methods are shown in Figures 17 to 24. The results

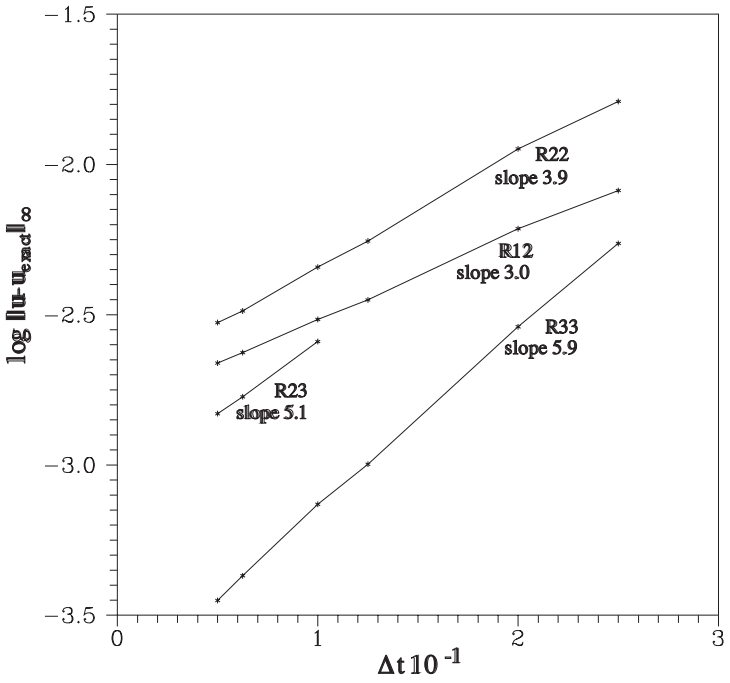


Figure 16: Order of convergence for the $R_{1,2}$, $R_{2,2}$, $R_{2,3}$ and $R_{3,3}$ schemes.

along the domain diagonal reported in Figures 17 and 18 are compared to the exact solution which is represented by discontinuous lines. Because a rather coarse mesh has been employed in the present test problem, the explicit methods could be operated with rather large time steps (80% of the critical value) and were found to be competitive with respect to the implicit methods as regards the computing time needed to complete the problem.

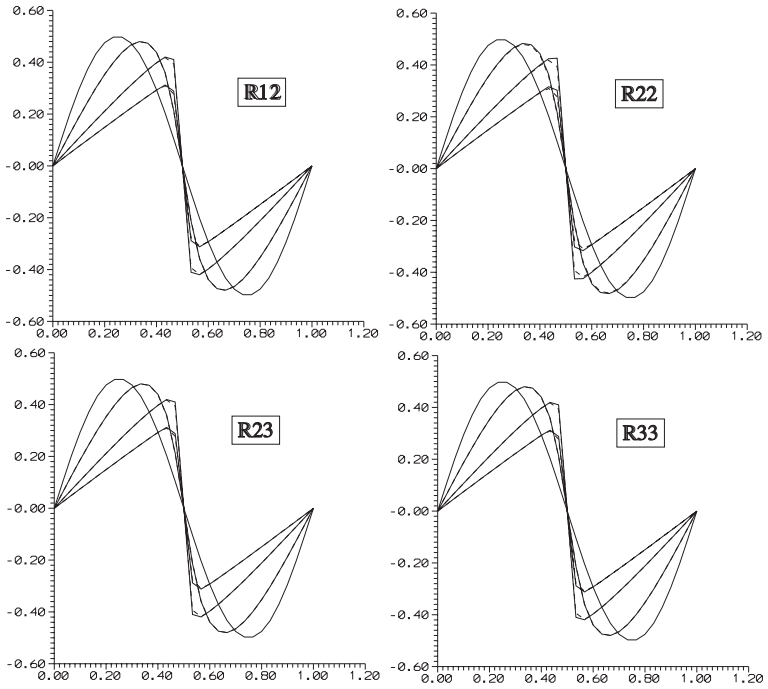


Figure 17: Solution $u(x,x,t)$ of 2D Burgers problem by $R_{1,2}$, $R_{2,2}$, $R_{2,3}$ and $R_{3,3}$ with $Pe = 3.33$, $c = 3$, $d = 0.9$ for $t = 0,\ 0.2,\ 0.6,\ 1$.

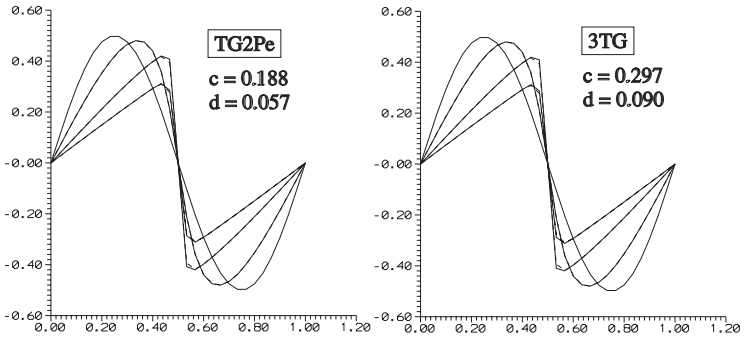


Figure 18: Solution $u(x,x,t)$ of 2D Burgers problem by $TG2Pe$ and $3TG$ with $Pe = 3.33$ for $t = 0,\ 0.2,\ 0.6,\ 1$.

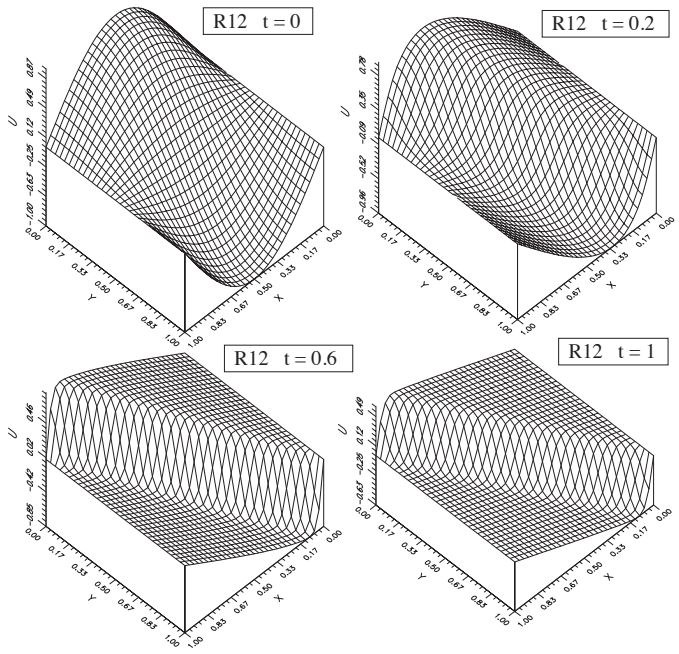


Figure 19: Solution $u(x, y, t)$ of 2D Burgers problem by $R_{1,2}$ with $Pe = 3.33$ for $c = 3$, $d = 0.9$.

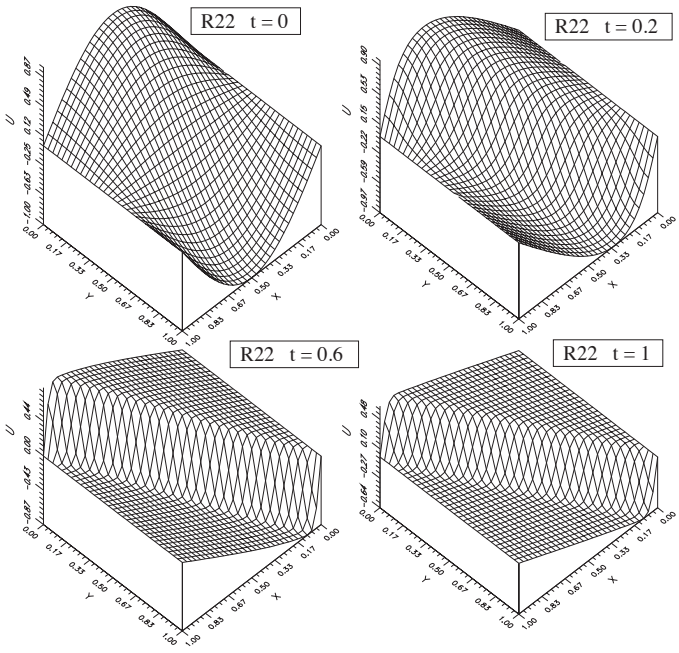


Figure 20: Solution $u(x, y, t)$ of 2D Burgers problem by $R_{2,2}$ with $Pe = 3.33$ for $c = 3$, $d = 0.9$.

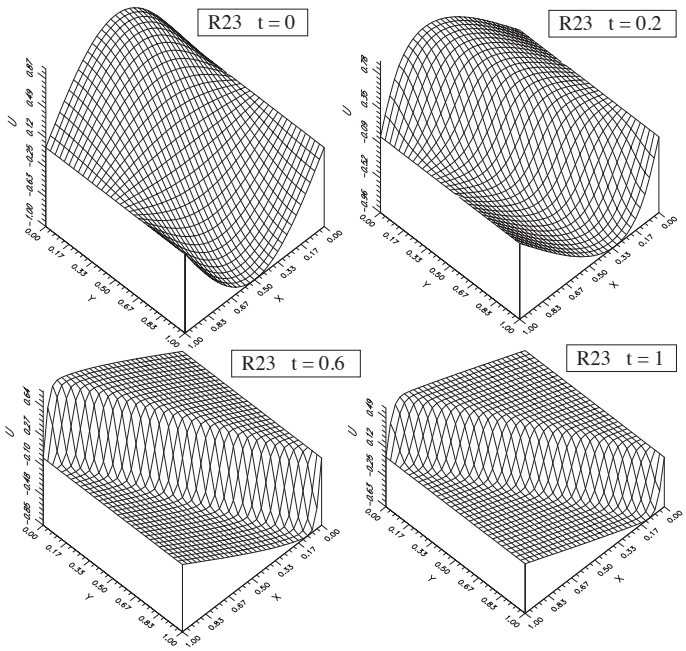


Figure 21: Solution $u(x, y, t)$ of 2D Burgers problem by $R_{2,3}$ with $Pe = 3.33$ for $c = 3$, $d = 0.9$.

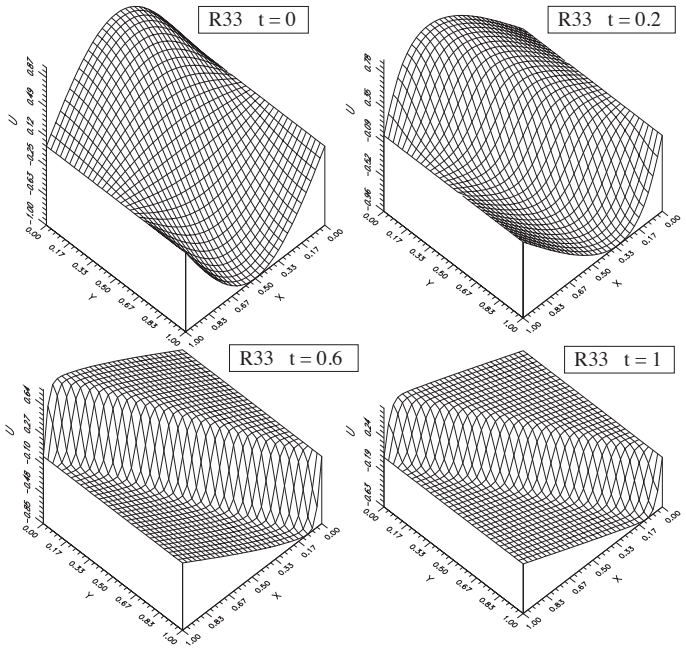


Figure 22: Solution $u(x, y, t)$ of 2D Burgers problem by $R_{3,3}$ with $Pe = 3.33$ for $c = 3$, $d = 0.9$.

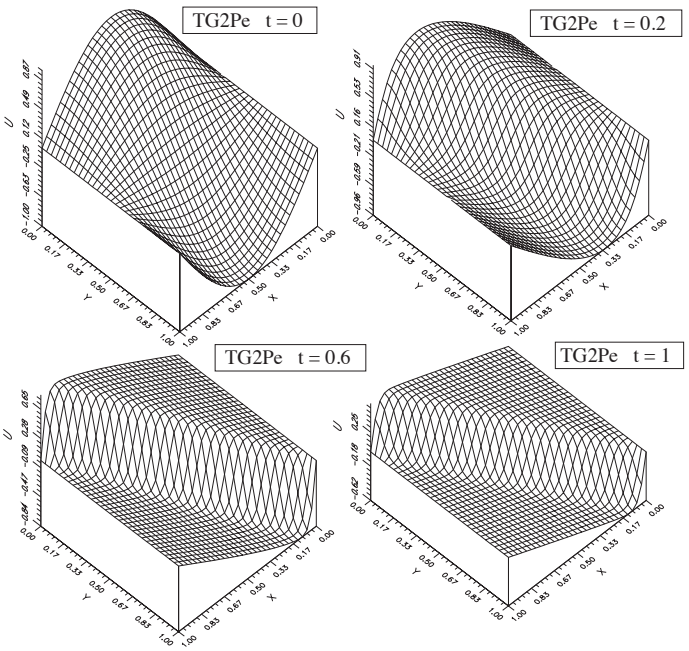


Figure 23: Solution $u(x, y, t)$ of 2D Burgers problem by $TG2Pe$ with $Pe = 3.33$ for $c = 0.18$, $d = 0.057$.

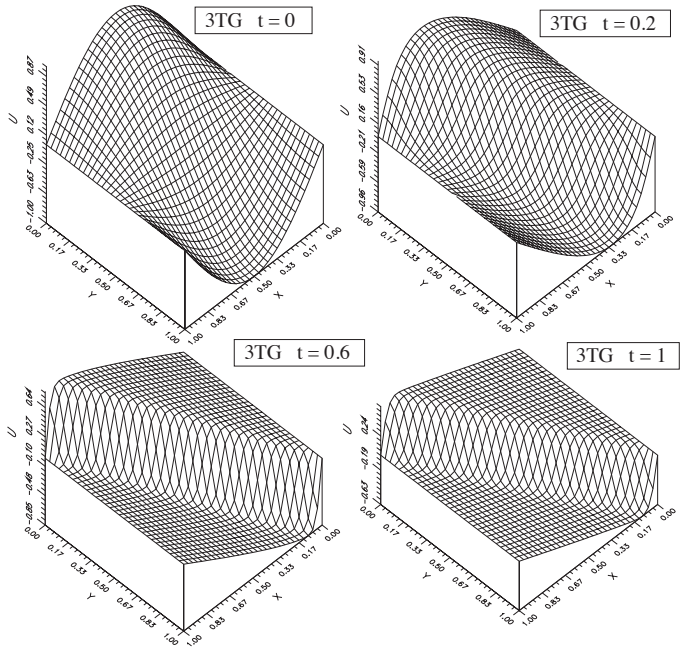


Figure 24: Solution $u(x, y, t)$ of 2D Burgers problem by $3TG$ with $Pe = 3.33$ for $c = 0.29$, $d = 0.09$.

# 6 Conclusions

A multi-stage approach to Padé approximations of the exponential function provides interesting explicit and implicit time-stepping methods of high order for tracing the transient response of convection–diffusion problems. Such methods only involve first time derivatives. This is an essential feature to enable the use of $C^0$ finite elements in conjunction with high-order time-stepping schemes in spite of the presence of a diffusion operator in the governing partial differential equation.

Moreover, the proposed implicit multi-stage schemes possess A-stability and good accuracy up to large Courant numbers. They are suited for transient problems and maintain their properties independently of the Péclet number.

The intimate relationship between multi-stage schemes derived from Padé approximations and Runge-Kutta methods has been underlined.

A least-squares approach which naturally introduces upwind-type weighting functions possessing the tensorial structure required to act only in the flow direction has been developed to ensure a stable spatial representation of highly convective situations.

Numerical tests, including an original 2D Burgers problem with analytical solution, have clearly shown that, when compared to traditional second-order time-stepping methods, the higher-order schemes permit the use of larger time-step values to reach a given time accuracy. Implicit methods of high order appear particularly competitive with respect to the more simple explicit methods in situations where the solution exhibits localized behaviour, thus requiring mesh refinement to achieve accurate results. In fact, explicit methods often break down in such situations due to their restricted conditions of numerical stability. Indeed the cost per time step of the high-order implicit methods is very much increased with respect to traditional second-order methods. Nevertheless, the numerical experiments performed so far indicate that they are definitely competitive with respect to traditional low-order methods.

Acknowledgements

The present study has been performed during a scientific visit of the first author to the Departament de Matemàtica Aplicada III of the Universitat Politècnica de Catalunya. The support of the Spanish Ministry for Education and Science, which made such visit possible, is gratefully acknowledged (grant number: SAB95-0426).

# References


[1] K.W. Morton, *Numerical Solution of Convection-Diffusion Problems*, Chapman and Hall, London, 1996.

[2] M. J. P. Cullen and K. W. Morton, 'Analysis of evolutionary error in finite element and other methods', *J. Comput. Phys.* **34**, 245–267 (1980).

[3] J. Donea, 'A Taylor–Galerkin method for convective transport problems', *Int. J. Numer. Meths. Eng.* **20**, 101–120 (1984).

[4] J. Donea, L. Quartapelle and V. Selmin, 'An analysis of time discretization in the finite element solution of hyperbolic problems', *J. Comput. Phys.* **70**, 463–499 (1987).

[5] J. Donea and L. Quartapelle, 'An introduction to finite element methods for transient advection problems', *Comp. Meths. Appl. Mech. Engrg.* **95**, 169–203 (1992).

[6] B.K. Swartz, 'The construction of finite difference analogs of some finite element schemes', in *Mathematical Aspects of Finite Elements in Partial Differential Equations*, C. de Boor (ed.), Academic Press, New York, 279–312 (1974).

[7] V. Thomée and B. Wendroff, 'Convergence estimates for Galerkin methods for variable coefficients initial value problems', *SIAM J. Numer. Anal.* **11**, 1059–1068 (1974).

[8] J.H. Argyris, L.E. Vaz and K.J. Willam, 'Higher order methods for transient diffusion analysis', *Comput. Meths. Appl. Mech. Eng.* **12**, 243–278 (1977).

[9] J. Donea, B. Roig and A. Huerta, 'High-order accurate time-stepping schemes for convection-diffusion problems', Monograph CIMNE n.42, International Center for Numerical Methods in Engineering, Barcelona (1998).

[10] E. Hairer, S.P. Nørsett and G. Wanner, *Solving ordinary differential equations I, Nonstiff Problems*, Springer Series in Computational Mathematics, 1987.

[11] E. Hairer and G. Wanner, *Solving ordinary differential equations II, Stiff and Differential-algebraic Problems*, Springer Series in Computational Mathematics, 1991.

[12] J.D. Lambert, *Numerical methods for ordinary differential systems*, John Wiley & Sons, 1993.

[13] J. Donea, S. Giuliani, H. Laval and L. Quartapelle, 'Time-accurate solution of advection–diffusion problems', *Comput. Meths. Appl. Mech. Eng.* **45**, 123–146 (1984).

[14] R.D. Richtmyer and K.W. Morton, *Difference Methods for Initial Value Problems*, Wiley Interscience, 1967.

[15] C.B. Jiang and M. Kawahara, 'The analysis of unsteady incompressible flows by a three-step finite element method', *Int. J. Numer. Meths. Fluids* **21**, 885–900 (1993).

[16] K. Kashiyama, H. Ito, M. Behr and T. Tezduyar, 'Three-step explicit finite element computation of shallow water flows on a massively parallel computer', *Int. J. Numer. Meths. Fluids* **21**, 885–900 (1995).

[17] A. Harten and H. Tal-Ezer, 'On fourth order accurate implicit finite difference scheme for hyperbolic conservation laws: I. Nonstiff strongly dynamic problems', *Math. Comput.* **36**, 335–373 (1981).

[18] T.J.R. Hughes and A. Brooks, 'A multi-dimensional upwind scheme with no crosswind diffusion', in *Finite Element Methods for Convection Dominated Flows*, T.J.R. Hughes (ed.), ASME, New York (1979).

[19] T.J.R. Hughes, L.P. Franca and G.M. Hulbert, 'A new finite element formulation for computational fluid dynamics: VIII. The Galerkin/ Least-squares method for advective–diffusive equations', *Comput. Meths. Appl. Mech. Eng.* **73**, 173–189 (1989).

[20] J. Peraire, 'A finite element method for convection dominated flows', Ph.D. Thesis, Univ. College of Swansea (1986).

[21] G.F. Carey and B.N. Jiang, 'Least-squares finite elements for first-order hyperbolic systems', *Int. J. Numer. Methods Engrg.* **26**, 81–93 (1988).

[22] N.S. Park and J.A. Liggett, 'Taylor-least-squares finite elements for two-dimensional advection-dominated unsteady advection-diffusion problems', *Int. J. Numer. Methods Fluids* **11**, 21–38 (1990).